

**Anonymous Referee #1 Received and published: 18 March 2019**

*This manuscript is a product of hard working and written in detail. However, if it is written concisely it will be much better. I think if it is revised a bit with editing and by incorporating some provided information it will be considered for publication.*

We thank the reviewer for accepting the correction of this article; we appreciate his/her favorable opinion about the work. We agree with most of the comments and we provide next a point by point answer to the concerns presented.

**1- Page 1 Line 26:** *Re-write this sentence concisely: "Wave breaking creates a wellmixed region to the lee of the obstacle that induces flow separation; the generation of a dividing streamline between undisturbed flow above and trapped energy and flow analogous to hydraulics in the lower surficial branch (Smith, 1985b)."*

*We will now rewrite this sentence more concisely, as follows:*

*"Wave breaking creates a well-mixed layer to the lee of the obstacle, which generates a dividing streamline separating undisturbed flow aloft and trapped energy and flow analogous to hydraulics in the lower surficial branch (Smith, 1985b)"*

**2- Page 3-4 Section 1.1** *is a big with repeating same expression time to time. As this is a scientific paper shorten being on a specific on Mountain wave phenomena, hydraulic analog and relation with the Froude number.*

We agree with the reviewer. In this section we aimed to put in context the physics behind the studied phenomena and introduce the hydraulic analog. However, it is true that it could be repetitive in some way and too extensive. In the revised version we reduce this section.

**3- Page 4 Line 20:** *"Fr in (Eq3)" is it equation 3? If so, there is no relation of Fr. Correct it.*

We apologize for the misunderstanding, we wanted to refer to equation 1. We correct this typo in the revised version.

**4- Page 6 Line 20;** *Replace "rugosity" by surface roughness (m)*

We will replace the word rugosity by surface roughness (m) in the revised version, as per the reviewer's request.

**5- Page 7 Line 6:** *"wind episodes". Where is wind? Figure 2a and 2b say they are 850 hPa level temperature and sea level pressure and also there are no any wind arrows. So, include wind.*

In these lines we are referring to the synoptic setting leading to the Tehuantepecer wind event. As discussed in the text, the cold air mass moving south from north America is instrumental for the development of Tehuantepecers, which is why Figure 2 shows 850 hPa and sea level pressure in a very wide domain. Winds are better shown with much more detail, focusing on the Isthmus, in Figure 3.

**6- Page 9 Line 4:** *"Isthmus (Figure 3d)". There is no caption of Figure 3d. Add this including its exact position (lat./long) so that it will can be compared with aforesaid matters.*

We apologize for our mistake. In the revised version we include the caption for this figure where the lat and lon of the sounding are explicitly mentioned. There is a line from Figure 3d to Figure

3c pointing to the location (NP) where the sounding is performed, but it is barely noticeable. We will mark it more clearly in the revised version.

**7- Page 9 Line 5:** *“inversion existent at about 800hPa or 2500m”. Seems from about 2000 to 2500 m. correct this. Looks sounding has multiple PBL and discontinuous stratification which refers an importance of study of high resolution data sets. So, mention this kind of information to highlight your approach of methodology.*

Another reviewer has noted that more than an inversion it is an isothermal layer, also highly stable, but not really an inversion. We will correct this issue and also include a comment about the need for high resolution for a study of this event. We thank the reviewer for this suggestion.

**8- Page 10 Line 10:** *“The temperature profile in Fig. 3d evidences that the latter level. . .”. What does latter level mean as it is hard to understand? If you are referring a presence of stable layer below 2.5km Figure 3d shows there is a presence of static instability, not stability below 2 km. So, regarding this issue rewrite this.*

We meant “the temperature profile in Fig. 3d evidences that the 2500m height level corresponds with the depth of the cold air”. The profile is stable above this level, but much less so than in the layers below.

We agree that it can be confusing as written in the original text, we will rewrite this statement in the revised version. We will also add dry adiabats in the sounding in Fig 3 to help identifying stable layers.

**9- Page 10 Line 31:** *“Figure 6a plots the Froude number (Equation 1)” How did you find “ $\theta_0$ ” (method) to calculate N for Froude number? Please mention figure nos. in following sentences as it will be easy to follow these criteria:*

We mostly follow [1] [2] and [3] below. As per some other reviewer's request, we will now show the Fr number some distance upstream the obstacle. We calculate Fr using the average Brunt-Väisälä frequency and average wind speed for the layers from the surface to the level of similar elevation as the mountain. We will explain this clearly in the revised manuscript.

[1] Pokharel, B., Geerts, B., Chu, X., and Bergmaier, P.: Profiling radar observations and numerical simulations of a downslope wind storm and rotor on the lee of the Medicine Bow mountains in Wyoming, *Atmosphere*, 8, <https://doi.org/10.3390/atmos8020039>, 2017b.

[2] Pokharel, A. K., Kaplan, M. L., and Fiedler, S.: Subtropical Dust Storms and Downslope Wind Events, *Journal of Geophysical Research: Atmospheres*, 122, 10 191–10 205, <https://doi.org/10.1002/2017JD026942>, 2017a.

[3] Grubišić, V., Serafin, S., Strauss, L., Haimov, S. J., French, J. R., and Oolman, L. D.: Wave-induced boundary-layer separation in the lee of the Medicine Bow Mountains. Part II: Numerical modeling, *Journal of the Atmospheric Sciences*, p. 150904104933002, <https://doi.org/10.1175/JAS-D-14-0376.1>, <http://journals.ametsoc.org/doi/abs/10.1175/JAS-D-14-0381.1>, 2015.

**10- Page 10 Line 17-21:** *These conditions are: a mountain with steeper lee slope (1) (Figure no. ??) crossed by strong winds (> 15m/s) (2) (Figure no. ??) mostly normal to the barrier (3) (Figure no. ??). A stable layer above the top and less stable above that (4) (Figure no. ??) with cold air advection and large-scale subsidence to maintain the C2 ESDD Interactive comment Printer-*

*friendly version Discussion paper stability (5) (Figure no. ??) . Apart from this, reverse wind shear above (6) (Figure no. ??) and no cool pool in the lee (7) (Figure no. ??), is also desirable. These conditions are all perfectly met for both locations analyzed, as discussed previously, and indeed intense downslope windstorms occur in both cases.*

These seven conditions were all mentioned at some point in the previous discussions, but we agree with the reviewer in that it will be very informative to summarize here the figures that evidence them as a reminder. We will modify the text accordingly in the revised version of the manuscript.

**11- Page 10 Line 31:** *Where is Figure 6a as there is no label a, b, c of Figure 6. So, it is hard to follow.*

We totally agree, excuse us for the mistake. This will be corrected in the revised version.

**12- Page 14:** *Insert figure no. "c" in Figure 7. How about the subcritical flow before the supercritical flow? Did you observe it within your region of interest before the supercritical flow? If so mention them with a value of Froude number so that it could be better to relate how the subcritical flow was converted to supercritical flow as downslope wind.*

We will introduce the subfigure letter (c) in the caption. Concerning the second issue, we will show the Fr number upstream the mountain in the revised manuscript.  $Fr \approx 1$  for the highest mountain and  $Fr \approx 2$  for the lowest one. In both cases the Fr values are in the range indicating transitional conditions from subcritical to supercritical behavior in the flow, as discussed in section 1.1 in the Introduction. It is difficult to define a Froude number with the same meaning as in shallow water; we nevertheless observe subcritical flow behavior, in the sense that the flow thins and speeds up as it goes upslope in the case of the lower mountain (Fig 5a and 5g), but not so clearly for the higher one.

**Anonymous Referee #2 Received and published: 19 March 2019**

*The paper discusses simulations of one downslope wind event with the limited-area model WRF using multiple nests down to very high resolution (444 m). The study is mostly well written and interesting but needs some substantial editing. I also think it would gain a lot if an additional small sample of Isthmus events could be simulated and discussed (perhaps not using the innermost expensive WRF nest). Doing so would allow to inter-compare events and discuss similarities/differences. Still, the paper might be publishable without doing so.*

We would like to thank the reviewer for accepting to review this manuscript; we appreciate the positive view of the work. We believe that the modifications suggested will improve the manuscript.

We agree with the reviewer's suggestion in that details about additional Isthmus events could contribute to their better understanding. We have simulated other Tehuantepecer cases occurring in 2013 and we have seen downslope windstorms and hydraulic jumps developing in the mountains east of Chivela pass, as those shown in the paper. The one we selected is the most intense event of the year. We nevertheless prefer to just focus the study in one clear case, given that these phenomena have never been reported before in the area. We leave for future work a more careful study with a sufficient number of cases to investigate the variability these extreme events.

In the revised manuscript we will include in the conclusion section a comment about our preliminary results for other events and the need for a more comprehensive study with a sufficient number of cases to investigate the variability associated with these extreme phenomena.

Next, we address each of the minor concerns presented by the reviewer

*Additional minor comments:*

**1- Page 4, line 21: missing equation**

It is true, there is a mistake in this line. In this case we want to refer to Equation 1, which is the Froude number calculation. We will correct it in the revised version.

**2- P5, l2: Figure 2c missing**

Here we were referring to Figure 1b, where d04 and d05 domains are displayed. We correct this typo in the revised version.

**3- P6, l 13: 0.5 deg x 0.5 deg**

We agree, we will perform the suggested correction in the revised version.

**4- P6, l20: rugosity is surface roughness length**

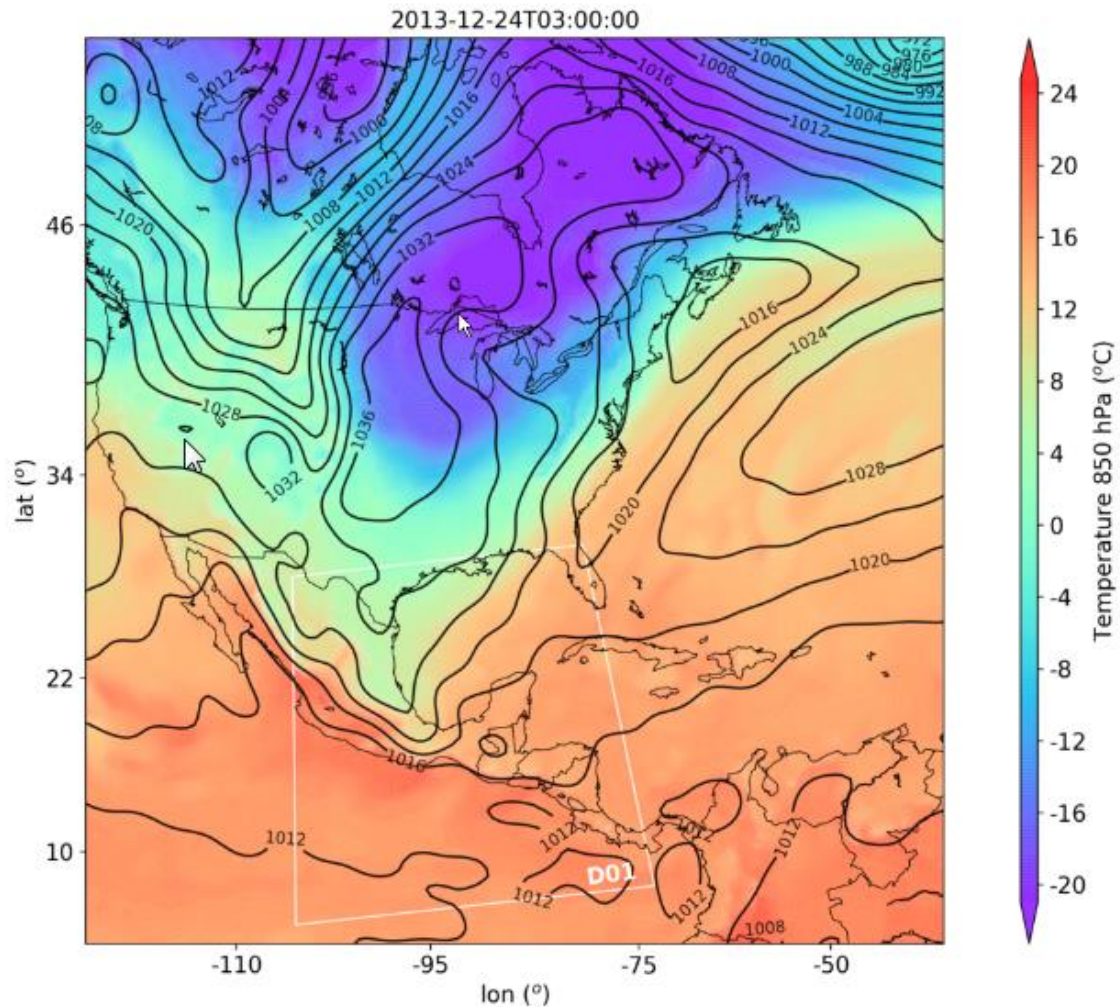
The reviewer is right; we will replace "rugosity" by "surface roughness length" in the revised version of the manuscript.

**5- Table 2: station elevations correct?**

Yes, it is correct, the elevations are low because both stations are on the coastal plain at the foot of the mountains. The observational data were provided by the Mexican National Laboratory of remote sensors. (<https://clima.inifap.gob.mx/Inmysr/Estaciones/MapaEstaciones>)

**6- Figure 2:** *Why before and after the event and not at peak intensity?*

A map similar to those in Fig. 2 but at peak intensity and focused on the Isthmus is shown in the ensuing figure Fig 3a in the paper. But we agree with the reviewer in that in Fig 2 it makes more sense to show the larger scale situation also at peak intensity than later during the episode. We will now replace Fig2b by the map below, corresponding to 24 December at 03 UTC.



**7- P9, I3:** *In the results section there should be no hypothesis ("which can potentially)*

We will correct the sentence (also including another reviewer's suggestion) as follows:

"As shown in the following section 3.2, acceleration on the top of these mountains and to their lee is related to gravity wave activity, which results in the development of strong downslope winds, rotors and hydraulic jumps."

**8- P9, I10:** *whose positions*

The correction will be made as suggested.

**9- P10, I20:** *Where can this perfect match be seen?*

The fulfillment of the listed conditions is supported by figures and discussed previously in the text. But we agree with the reviewer in that it should be reminded here. We will change the paragraph as follows:

“These conditions are: (1) an asymmetric mountain with steeper lee than windward side (Fig 5), (2) crossed by strong winds ( $> 15\text{m/s}$ ) (Fig 5), (3) mostly normal to the barrier (Fig.3, 5). (4) A stable layer above the top and less stable above that (Fig 3d, 6c), (5) with cold air advection and large-scale subsidence to maintain the stability (Fig 3d, 6c). Apart from this, (6) reverse wind shear above (Fig 3d, 6c) and (7) no cool pool in the lee (Fig 3a, 6b), is also desirable. These conditions are all perfectly met for both locations analyzed, as discussed previously, and indeed intense downslope windstorms occur in both cases.”

**10- Figure 5:** *It is difficult to understand what is what cross section? Mention "up1" in the caption.*

We agree with the reviewer. In the revised version we will indicate in the caption the meaning of UP1 and UP2. These points are the locations where we represented the upwind potential temperature profile (Figure 6).

**11- Figure 9b,c:** *Easier to compare if you use the same domains? Did you discuss the missing northern stratiform cloud deck in the simulations?*

We agree with the reviewer's consideration; it would be easier to compare Figure 9 b with Figure 9 c if we showed them in the same domain. However, it was not possible for us to obtain a clear satellite data representation for domain 05 only. The data used in Figure 9 is directly extracted and postprocessed from GOES-R raw database. We did our best to display the clearest possible image of the small lee cloud formation, and for this purpose we decided to zoom out this image so that the grey color scale is adjusted with the rest of the existent features (the other clouds, the lake and the sea) and the lee clouds appear more sharply defined . In any case, in the revised version we will add another panel zooming in to exactly match domain 05 for an easier comparison with the model results. Regarding the northern stratiform cloud deck indicated by the reviewer, it is hinted by the model (you can see the edges of it in domain 5 in Fig 9a), but it is likely not correctly simulated because it is only very partially included in the domain and cloud water is not part of the boundary conditions for nested grids. We will mention this in the revised version.

**Anonymous Referee #3 Received and published: 19 March 2019**

*General: This paper reports on simulations of terrain induced wind systems in Mexico, and is novel in the respect that I have not seen much work in this particular region. The question that I have been wrestling with is however: "Is this novel science?"*

*The simulations are carried out for one single events, and while the authors may feels this was a typical event, the reader is not given much information other than some verbal arguments. So this remains a case study, and does not even claim to be general. The type of flows that are described (mainly downs-slope wind-storms and hydraulic jumps) occur at many places around the world and has been studies extensively both from observations and with models. It is well known that numerical models perform well in these type of "hydraulic flows"; hence it does not reveal anything new about the flow features other than such that are directly related to specific local features. The authors do not even try to show that this type of flows have special characters because of the geographic location, which closer to the equator than in most other studies.*

*Hence, there is nothing new here and from that respect I should have recommended "reject". However, there is nothing fundamentally wrong with the study as such, so maybe that would be unfair. So I will leave to the editor to determine if the world needs one more paper about these events. I would tend to say "no", but in the case the editor say "yes" the paper still needs major revision.*

We thank the reviewer for accepting the evaluation of this manuscript; we appreciate the effort of his/her thorough review. The reviewer's general concern about the significance of our research to the existent science in the field is well taken; perhaps we have not made our contribution apparent enough in the text. We consider that the manuscript has several outstanding points that make it a noteworthy publishable work for this journal:

1) It is true that Tehuantepecers are orographically induced flows, of the kind occurring elsewhere on the planet. They are, however, of the very few with a global significance. Winds funneled through the Isthmus of Tehuantepec, are so intense and extend so far out to sea, that they are clearly visible from space, in scatterometer data, microwave derived total precipitable water, and even forming large rope clouds in their outflow/frontal boundary. Furthermore, Tehuantepecers produce strong upwelling in the Gulf of Tehuantepec resulting in large chlorophyll blooms that are critical for the food chain and marine life in the eastern Tropical Pacific. So, they are not just one more of this type of flows.

2) The scope of the paper is not to demonstrate anything particularly special about these orographic flows in terms of physics. Instead, our research's goal is to show that intense flow acceleration in the Isthmus of Tehuantepec during Tehuantepecer events is not restricted to the well-known mountain gap wind jet off Chivela pass, but occurs in the neighbouring Sierras as well, in a stretch of over 100 km and for different dynamical mechanisms, forming downslope windstorms and hydraulic jumps. Our research objective is scientifically relevant because, while much attention has been given to the gap winds through Chivela pass, very little is known about the flow structure and associated extreme phenomena developing elsewhere across the Isthmus. Our work is the first, as far as we know, to analyze these extreme winds and discuss their driving dynamics.

3) Knowledge about these phenomena is also important for social and economic reasons because of the major impact that they have on the region. These extreme events cause, every year, problems and accidents involving population as well as infrastructure (please, see the references in the Introduction section), and a better understanding about them can help to mitigate the damages that they produce. Moreover, the region is the most important for wind energy generation in all of Latin America. These events directly affect the production of wind turbines and could undermine their performance if not considered in wind farm operations.

In the new version of the manuscript we will bring out more clearly the goal of our study and why it is novel science (point 2 above), building upon previous studies on Tehuantepecers.

Tehuantepecers are a recurrent feature of the circulation in the area, particularly in winter months, as we explicitly mention and support with references in the Introduction section. We simulated other events during late 2013 and also the previous winter season in early 2013, and we saw that downslope windstorms and hydraulic jumps also develop in the flow across the Isthmus. The case we present in the paper is the most intense and long lasting in the period, but we are very certain that the occurrence of these extreme phenomena is commonly associated with Tehuantepecer events in general. Evidences come not just from our model data, but also from wind company reports and from the damages they cause.

With regard to the use of a model for the study, it is of course not a novelty and we do not claim it to be so at all in the paper. It is precisely because models perform well in simulating these orographic flows, as the reviewer mentions, that we use one to analyze the flow structure and explain the particular mechanisms producing downslope windstorms and hydraulic jumps in the area. Unfortunately, there are no direct observations to help with the task, so a model is the best approach we can find.

*I have two main concerns:*

*1) The analysis of the model results is rather superficial and makes many claims that are hard to substantiate from the graphic material presented. I'm sure this could be turned into a nice paper if the authors try to think a bit out of the box and perform an actual analysis of the model results, rather than just produce a few standard plots direct from the model data. Much of the theoretical background includes the planetary rotation; this is not commented on at all and here may be an opportunity to take a novel angle, comparing these results to higher-latitude cases. Just in general I would like to see a more in-depth analysis.*

The Rossby number for the flows in our study is high (above 13), given the small width of the mountains (about 35km in both cases), the strong wind speed of the order of 20m/s and the low latitude ( $f$  is about  $4 \times 10^{-5}$  rad/sec, less than half the value in midlatitudes). The role of planetary rotation is therefore very minor when compared with the effect of inertia, pressure and gravity forces. Mountain waves and related orographic flows such as those producing downslope windstorms and hydraulic jumps are in general high Rossby number motions everywhere, even at much higher latitudes; thus, in all related theoretical studies we know of (certainly in all those cited in the paper), the Coriolis force is neglected.

However, the effect of planetary rotation, or rather the lack of it, is indeed very relevant to explain the large extent over the ocean of the accelerated flow exiting the Isthmus. As mentioned above, the latter is instrumental to make Tehuantepecers stand out for their size and impacts among other orographic flows. Is it, perhaps, this effect what the reviewer's concern is about?

Gap winds and downslope windstorms in mid and high-latitudes do not usually extend too far downstream from the mountains where they develop; the exiting accelerated flow adjusts quickly to the general geostrophic synoptic flow in the region. Even in gap winds through marine straits, where the exit region is free from topographic obstacles as in Tehuantepecers, the outflow weakens and merges with ambient circulations in relatively short distances. The article by Steenburgh et al (1998), cited several times in the text, discusses the mechanisms behind the large downstream extension of Tehuantepecers over the Gulf of Tehuantepec arguing that it is the combined effect of the lack of obstacles on the marine surface and the low  $f$  parameter of the tropical latitude of the area. The small Coriolis force results in very weak synoptic circulation (small pressure gradients and low wind speeds) and hence the gap wind does not encounter any ambient large-scale flow to merge with, describing a very-close-to-inertial trajectory. Furthermore, a small Coriolis force produces weak wind deflection and thus the anticyclonic curvature of the gap jet as it moves over the ocean is not very pronounced. These authors perform numerical experiments for the Tehuantepecer case they studied with the  $f$  of  $45^\circ$  N and show that in mid latitudes the gap wind outflow would curve much more westward, thereby not reaching as far south as in the actual situation.

Another result in the numerical experiments in Steenburgh et al. (1998) with different  $f$  values, is that the gap winds and flow in the Isthmus itself are largely unaffected by changes in the magnitude of the Coriolis parameter. Therefore, as theory predicts, planetary rotation plays only a minor or negligible role in the development and dynamics of these orographic circulations.

As per the reviewer's suggestion, we will comment on planetary rotation and the impact of the low latitude in Tehuantepecer's structure (mostly on the extent of the outflow in Gulf of Tehuantepec) in the Introduction section of the revised manuscript, and also when discussing the large reach of the accelerated flow resulting from the downslope windstorm in the lowest mountain in our analysis.

**2) *The main results are all together expected and reveals nothing about this flow that couldn't have guessed without the model simulations. Sure there are details here that no one could guess, but much of that detail is not harvested.***

We disagree. We haven't seen any mention of downslope windstorms or hydraulic jumps developing in the Isthmus in any study related to Tehuantepecers, not even in the highly referenced article by Steenburgh et al. (1998), discussed above, detailing the dynamics of the gap winds and their outflow over the Gulf of Tehuantepec with the use of numerical simulations. If it was so evident that the flow shows the behavior we analyze in our work, it would have been reported in some of the several studies dealing with Tehuantepecers. The focus is always on the gap wind jet off Chivela pass. In Steenburgh et al. (1998) there is only a very brief comment about mountain waves and flow acceleration occurring also on the lee slope of the mountains east of Chivela pass, where their trajectory analysis shows that the cold air is also able to cross over to the Pacific side of the Isthmus, but with no further elaboration. The reason is likely related to the low resolution (6.67 km) or to the now outdated MM5 model used in this early study, which were not capable of simulating the downslope windstorm and hydraulic jump phenomena. Thus, this provides evidence that high resolution simulations with an adequate tool (the WRF model) are indeed necessary to reveal these flow features. They are certainly not captured by global analysis and there are virtually no station observations or observational campaigns that can disclose their existence and structure.

*Finally, the language would benefit from editing by a native english speaker.*

We will ask a native speaker to edit the manuscript, as per the reviewer's suggestion.

Specific:

**1-** *Make sure you define abbreviations the first time you use it, and stick with abbreviation afterwards. HJ is not explained, and is used interchanging with "hydraulic jump".*

This is true, we will correct this in the revised version of the manuscript.

**2-** *Drop the entire section 1.1; this is textbook stuff and just take up space.*

Section 1.1 aims to put in context the hydraulic analog theory applying to the studied flows. We considered it important because it helps to better understand the discussions, as we often refer to this theory throughout the article. However, we understand the reviewer's concern, and in the revised manuscript we will reduce this section.

**3-** *If you feel a need to validate the model, this should come before results, not after. Moreover, the cloud evaluation is superficial to the point of being useless. Either drop it or develop it.*

The validation we are performing is not a general validation of the model, since there are very few observations (just two sites) and not exactly in the best locations in relation with the phenomena we are studying. To begin by validating d04 and d05 even before explaining what we are analyzing, could confuse the reader and make explanations and discussions difficult to follow. It seems more appropriate and natural to us to first analyze the model results and then verify that they indeed agree with point observations.

With regard to the cloud evaluation, we do not think it is useless at all. That lee wave clouds exist in the same location and with the same extent as in the model results, strongly suggests that the model solution is accurate in simulating trapped lee waves precisely in the focus area, and therefore realistic. In the revised version of the manuscript, we will show the cloud image and model results over the same exact domain, to make comparisons easier and highlight the value of this piece of evidence.

**4- P3, I25:** *What do you mean by microscale?*

We mean atmospheric motions of spatial scales less than 2km, following the definition of microscale in the American Meteorological Society (AMS) glossary of meteorology. The resolution of the innermost grid is 444m, sufficient to resolve some of these motions, including rotor circulations and even the hydraulic jump itself. However, since we are really referring to details of the downslope windstorms, while microscale meteorology is most often dealing with turbulence and other truly small-scale processes, we are going to change the word microscale and rephrase the line:

*"In section III, the primary results obtained are shown, divided by the synoptic-mesoscale situation, the upstream-downstream structure of the phenomena and the microscale situation"*

By:

*"In section III, the primary results obtained are shown, divided into synoptic-mesoscale situation and upstream-downstream structure of the phenomena"*

The word microscale in the line the reviewer is referring to is actually correct, since the WRF model can run in L.E.S (large eddy simulation) mode resolving turbulent eddies, which are indeed microscale motions.

**5- Figure 1:** *Why are the two most high-resolution domain off center wrt to the gap?*

Precisely because the focus of our study is not the flow through the gap (Chivela pass) but in the mountains around, especially those to the east. Perhaps we didn't make it apparent enough in the article. We will modify the Introduction section, as mentioned above, to highlight more clearly the goal of our work, and what sets it apart from previous literature on Tehuantepecer winds.

**6- P6, I3:** *How much of a spinup is required before the model physics is realistic?*

From 3 to 6 hours is usually recommended. This is a standard practice in WRF simulation with this resolution [1]. Downslope windstorms and hydraulic jumps form around 12 UTC December 23, which is when we start the simulations. We show results from 3h into the simulation in Figure 5 only, to illustrate how the phenomena that we want to study develop. Most of the analysis is from data with a spinup time of 15h and more, when the flow features are fully mature.

[1] Warner, T. T. (2011). Quality assurance in atmospheric modeling. *Bulletin of the American Meteorological Society*, 92(12), 1601-1610.

**7- P6, I18:** *This is incorrect;  $U^*$  is not a wind speed; its a scaling parameter that depends on the vertical turbulent momentum flux. Also explain how the logarithmic wind-law is applied; with this formula, the wind just increases with height, so you need an anchor point.*

We agree with the reviewer in that  $U^*$  is not a real velocity but a parameter related to the vertical turbulent momentum flux. It is a reference velocity or a velocity scale, whose square value yields the magnitude of the vertical turbulent momentum flux near the surface, where it is assumed to be independent of height and nearly constant. It has dimensions of velocity (units are m/s) and it is called friction velocity in all text books and literature we know of. Perhaps the reviewer concern is related to the  $w_s^*$  symbol we used in the text, which can be confused with a real wind speed, such as  $w_{sz}$ . We will change the  $w_s^*$  naming for this parameter in Equation 3 to the more standard  $U^*$  symbol, so that no confusion can be made with an actual windspeed.

**8- Figure 2:** *What is the height of the 850 hPa wrt mountain crest? Why pressure levels at all, and not model levels? Note the warmest temperatures hanging on the southward facing lee slope; DSWs already happen here? Maybe the D01 domain is a bit small, or could have been located farther north, since there's a lot of uninteresting ocean south of the coast.*

Figure 2 displays the synoptic setting for the Tehuantepecer event in our study. It is not depicting model results, but global analysis data at 25km resolution. The use of pressure levels is a standard practice for this type of plots. We show 850 hPa temperatures and surface pressure because we are interested in the situation at low levels. The purpose of the figure is to illustrate how the low-level cold air driven by cold air damming in the Rockies continuing in the Sierra Madre Oriental in Mexico, moves fast southward, reaching the Bay of Campeche. The 850hPa surface is around 1600m in Mexico, within the cold air mass, which tops at about 2500m (see the sounding in Fig 3d). The tallest mountain crests in the Isthmus are around 2000m.

We do not see any sign of DSWs in these images; there is not enough detail, and as the reviewer suggests, a map in pressure levels might not be the most appropriate for the task.

The D01 domain is centered in the Isthmus. It includes a significant marine portion in the south because of large extent of the Tehuantepecer outflow into the ocean, as the reviewer can observe in Figure 3a. It is convenient to set the boundary relatively far downstream from the area of interest to avoid numerical problems related to the imposed lateral boundary conditions, such as wave reflections that can perturb the solution within the domain.

**9- Figure 3:** *Results are impressive but not unexpected. Moreover, legend for panel (d) is missing.*

We are glad that the reviewer finds these results impressive. They might be expected for someone with the level of expertise of the reviewer, but we believe that the general audience of the journal and especially those with interests in the area will find them revealing.

The missing legend for panel (d) will be included in the revised version. Thank you for noticing.

**10- P8, I8:** *What is the Rossby radius of deformation here.*

If we consider the depth of the surge to be around 2500m and the Brunt Väisälä frequency  $0.012 \text{ s}^{-1}$ , the Rossby radius of deformation is approximately 750 km. For comparison, the Isthmus is about 200 km across.

Clarke (1988) argued that since pressure gradients are so weak over the Gulf of Tehuantepec, the wind should follow a close to inertial trajectory. The radius of this inertial path for an outflow velocity of 25 m/s and 15N latitude is 662 km, which appears to be in the range of what we see in our simulations, at least along the main outflow axis, where the cross-flow pressure gradient is very small. Steenburgh et al (1988) found this to also be the case, as they discuss in detail the balance of forces for the gap outflow over the Gulf of Tehuantepec, explaining its fan like structure and curvature. In our work, as noted before, the focus is not on the gap outflow, but on the smaller scale extreme wind phenomena occurring in the Isthmus. We will, nevertheless, mention the reasons for the outflow's shape in the introduction section when briefly commenting on the effect of planetary rotation (see response to main concern 1, above).

Clarke, A. J., 1988: Inertial wind path and sea surface temperature patterns near the Gulf of Tehuantepec and Gulf of Papagayo. *J. Geophys. Res.*, 93, 15 491–15 501

**11- P8, L9:** *Are you here referring to the cross-over in the T-shaped structure? Might this is the DSWs? There seems to be a tremendous along-flow convergence/divergence here.*

Yes, exactly, we are referring to the strong flow acceleration represented in Figure 3b, with a T-shaped structure. As we show in detail later on, this is where the DSW occurs.

**12- P9, I2:** *Here you argue that this is a "flow thinning" event and not a gravity-wave breaking downs-slope flow event, but later it is the opposite.*

The flow thinning we are referring to here is that occurring under the dividing streamline generated by gravity-wave breaking to the lee of the mountain. We will remove "flow thinning" from this sentence to avoid confusion with the one happening for example in the case where there is an inversion layer close to the mountain top.

**13- P9, I4:** *And where is NP? Moreover, this analysis (d-panel) would have been much more informative if you had analysed the depth of the cold air and plotted it as a contour plot, showing its geographical distribution*

We agree with the reviewer's suggestion, in the revised version we correct Figure 3, better explaining where NP point is and introducing the caption for Figure 3d. Figure 3d contains more

information than just the depth of the cold pool, which is relatively homogenous in the area, as seen for example in Figures 6b and 6c. It shows the stability of the column and the vertical wind profile. We prefer to maintain the current panels in Figure 3, but we will add a comment about the depth of the cold air in position NP being similar to that closer to the mountains.

**14- P9, I5&6:** *If you want to use this type of sounding plot, you need to tell the reader what's on the axes. If the gray transverse lines are isotherms, there is hardly any inversions at all; to me the lower one looks more like an isothermal layer while the upper (subsidence) may be a weak one.*

The plot is a skew-T log-P diagram, very commonly used to represent upper level soundings and quite standard in weather analysis. Perhaps it may be confusing that it is lacking wet and dry adiabats? We will add the dry ones, which are relevant for the discussions. We will specify it is one of such diagrams in the text and add further details about the barbs in the wind profile and their scale, which is missing in the caption.

The reviewer is right in that the inversions are fairly weak, especially the lower one. We will replace the wording “shows the depth of the cold air pool, defined by the inversion existent at about 800hPa or 2500m in the temperature profile” by “shows in the temperature profile a stable lower boundary layer capped by a very stable isothermal layer from 850hPa up to about 800hPa, or 2500m, defining the depth of the cold air pool”

We will also change the word “inversion” by “very stable isothermal layer” in other instances of the text discussing the depth of the cold air pool.

**15- P9, I19:** *Awkward; what do you mean by "far reaching"?*

We mean “reaching out as far as the mountain gap winds do”. In the revised version of the manuscript we will rewrite this sentence to make it clearer for the reader.

**16- Figure 4:** *Show the modeled wind speeds already here and save a plot later*

With this figure we want to show the whole Tehuantepecer event duration (from the 23<sup>rd</sup> of the December to the 29<sup>th</sup>), as reflected by the observations. We also show some days before and after to contrast Tehuantepecer winds with the typical flow regime in the area. Furthermore, the figure provides justification on the period chosen for analysis as the 36h interval of maximum intensity (highlighted in both observational timeseries). We consider that including model results here for the purpose of validation would distract the reader by making the figure rather messy, so we prefer to leave it as it is, and keep the validation in a separate figure for a shorter interval allowing much more detail.

**17- Section 3.2:** *drop first sentence; we just read about that, no need to repeat.*

We agree we reviewer's comment, in the revised version of the article we will drop this sentence.

**18- P10, I67;** *Awkward English; what is a "wind path"?*

We mean “encompassing the flow path before and after crossing the mountains”, we will correct this in the revised manuscript.

**19- P10, line 19;** *"steeper" than what?*

We wanted to say: ‘asymmetric mountain with steeper lee than windward side’, we will change this in the revised version.

**20- P10, I23-24** and elsewhere: *I don't dispute the wave-breaking argument, but how can you see this here? There are no temperature-gradient reversals that I can see, nor is there any TKE aloft that would result from it. I would have expected to see at least truly vertical isotherms and elevated layers of TKE, or gradient reversals and no TKE.*

Vertical isentropes are more clearly seen at early stages and in the case of the higher mountain (see Fig 5d), but they are also present in Fig 5a for the lower mountain. They occur in the area that appears dark blue later on (Fig 5g and 5j) showing very low or close to zero windspeeds, and where isentropes are split apart from each other, indicating a well-mixed region. Overturning isentropes and temperature-gradient reversals are observable in the case of the higher mountain only, in Fig 5d. We will include as supplementary material an animation of figures like those in Fig 5 to show the process of development of the DSWs. In the animated sequence wave breaking is more apparent.

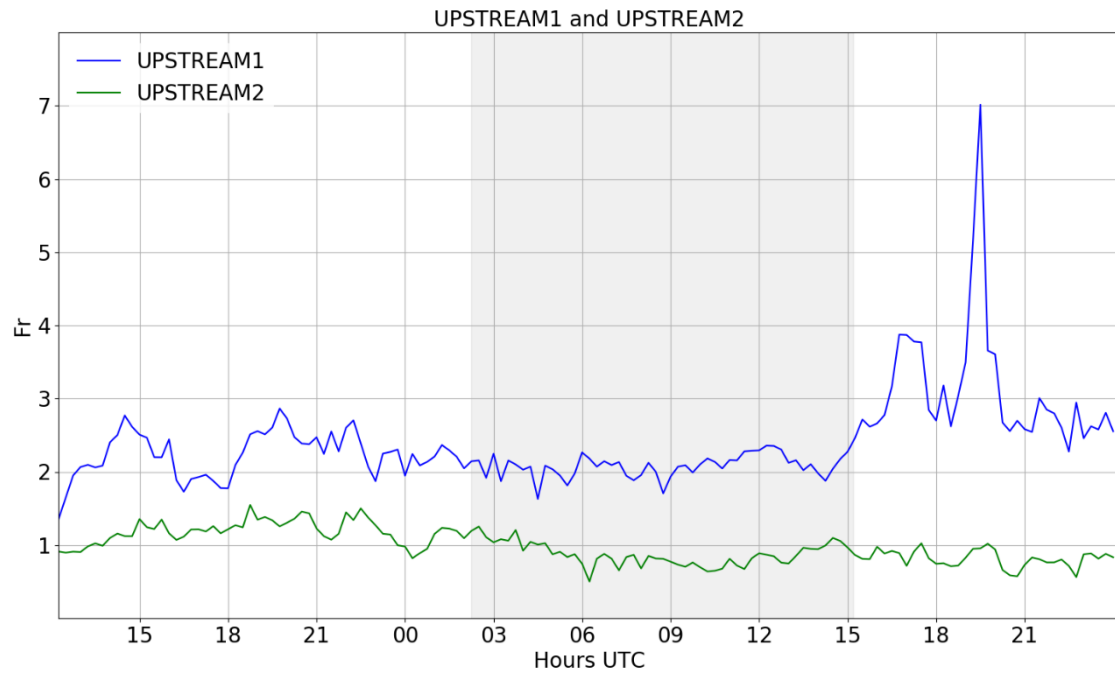
We agree with the reviewer in that there should be higher TKE values in the same layers where wave breaking occurs, but this variable is the result of the PBL parameterization in the model and thus it only considers subgrid scale variations in wind speed due to turbulent eddies, as represented in the scheme. The turbulence due to wind shear in the column is well captured; however, the turbulence associated with gravity waves, due to rotors and non-local turbulence advection is not represented and accounted for, because a much higher horizontal resolution of the order of tens of meters would be needed. This problem in numerical models is well known (see for example the review paper by Vosper et al. 2018) and we will introduce a comment about it in the revised version of the manuscript.

Simon B. Vosper, Andrew N. Ross, Ian A. Renfrew, Peter Sheridan, Andrew D. Elvidge and Vanda Grubišić, 2018: Current Challenges in Orographic Flow Dynamics: Turbulent Exchange Due to Low-Level Gravity-Wave Processes. *Atmosphere*, 9, 361. doi:10.3390/atmos9090361

**21- P10, I28:** *What do you mean by "bounded by turbulence"?*

We are describing Figure 5i disposition of TKE highest values, in shaded green. We mean "confined by layers of strong wind shear and turbulence", we will reword the sentence in the revised text.

**22- P10, I31** *The use of Fr is a powerful but yet blunt instrument to analyze these flows. I have two concerns here: 1) As the air has propagated up til crest of the terrain, Fr is already modified. The classical analysis by Durran, cited earlier, also uses the upstream Fr before the flow has hit the terrain; not that at the top of the hill. Hence I would have liked to see the truly upstream Fr instead; not the value that has already been modified. 2) Is it certain that the air reaching the observation stations actually comes from the point directly north of the station? A trajectory analysis would clarify the 3D dynamics of the flow.*



The figure above shows the Froude number at upstream points 1 (low mountain) and 2 (high mountain). The values are not so different from those shown in the paper, with  $Fr$  close to 1 upstream of the high mountain where the strong HJ forms and around 2 in the case of the low mountain. We will now include the calculation of  $Fr$  upstream instead of at the top of the mountain as per the reviewer's suggestion.

With regard to the question about the upstream trajectory of the air reaching the observation stations, we do not fully understand the reviewer's concern. The wind is from the north and quite steadily at low levels, so we consider that the cross sections in the north-south direction serve very well the purpose of showing the vertical structure of the flow as it crosses the mountains.

**23- Figure 5:** *To much information in too many too small panels. In fact, you could easily get rid of one third, by plotting the TKE and  $w$  in the same panels, as you do with temperature and winds.*

Because of the relation between TKE and wind shear we would prefer to keep the panels showing both TKE and wind speed contours. Adding vertical velocity as an extra layer would make them very difficult to read. We think that is best to keep Fig 5 as it is, unless the reviewer has a very strong objection. With its high resolution, the figure can be readily expanded to reveal all fine scale details very clearly.

**24- P11, 11:** *The position of the hydraulic jump, which is far from very distinct to begin with, hardly makes any propagation clear. Instead, analyze the position of the jump at different times and plot the position, and maybe also its strength, as a function of time. Maybe also as a function of  $Fr$ . From this the reader cannot really see any propagation.*

The small hydraulic jump lies around latitude 16.40 in Fig5a, but it is only easy to spot if one sees the sequence in motion. We will now point at the animation in the supplementary material (see response to comment 20 above) instead of Fig5a alone when commenting on this modest hydraulic jump.

**25- P12, line 1** Use "indicating" instead of "signalling"

We agree with reviewer's suggestion. We will use "indicating" in the revised version of the article.

**26- P12, l5;** "further high" is awkward.

The sentence "Stability is much reduced further high,..." will be rewritten as "Stability is sharply reduced aloft..."

**27- P12, l9:** Can't see any wave overturning in these plots. This may be because mixing erodes overturning isotherms before they can be seen in the model output. In that case there should be TKE there, which I can't see either

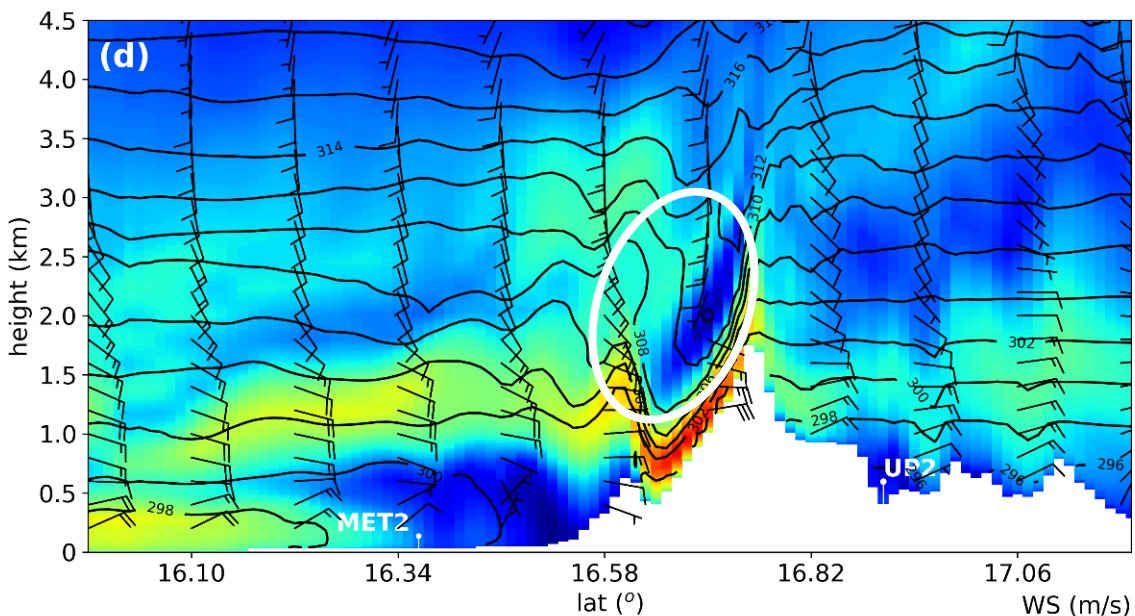


Fig 5 d from the paper is shown above with a white oval highlighting isotherm overturning, clearly visible for  $\theta = 308$  K and  $\theta = 310$  K to the lee of the mountain. We will add a similar marking in the revised manuscript.

The reviewer is right in that mixing erodes isotherm overturning very quickly, both with resolved vertical motions responding to the created instability and by subgrid turbulent eddies from the PBL scheme. The TKE variable is only reflecting the latter contribution; therefore, it has a smaller value than it should. In addition, the PBL scheme is more designed to account for convective instability and turbulent eddies rising from the surface due to heating, than to deal with instability resulting from gravity wave overturning, like what we see here. Thus, it is also underestimating TKE in this case. As mentioned in the response to comment 20, this is still an open issue in numerical modeling. We will add a comment about it in the revised version of the manuscript.

**28- P12, l30:** Awkward; "slightly ... d05".

We agree with reviewer. In the revised version, we replace the sentence "...slightly better so those from d05,..." by "...slightly better in d05 case ..."

**29- P12, l34:** Also awkward; "which situations".

We will replace "which registers HJ situations" by "downwind from the strong HJ"

**30- *Conclusions contain far reaching statements that cannot be substantiated by one case study***

We will tone down some of the concluding statements. In particular, we will remove the ending sentence "It is likely that the depth of the cold pool and how it compares with topographic barrier height, is a key factor determining the extent, location and intensity of these lee wave phenomena and whether they take place at all", which we agree it is unsubstantiated from just one case study.

**List of relevant changes made in the manuscript:**

- 1- Title.
- 2- Abstract: extra explanation.
- 3- Introduction: typo corrections.
- 4- Introduction: several concepts better explained.
- 5- Introduction: reorganization of some parts.
- 6- Introduction 1.1: summarize subsection, length of the text reduction.
- 7- Methodology: typo corrections.
- 8- Methodology: several concepts better explained.
- 9- Methodology: Equation 3 corrected.
- 10- Results and discussion: typo corrections.
- 11- Results and discussion: new Figure 2b.
- 12- Results and discussion: Figure 3d improved.
- 13- Results and discussion: several concepts better explained.
- 14- Results and discussion: Figure 5 modified and caption corrected.
- 15- Results and discussion: Figure 6a new plot representation. Figure 6bc improved.
- 16- Results and discussion: Figure 9 improved.
- 17- Conclusions: typo corrections and small reduction at the end.

# Downslope windstorms in the Isthmus of Tehuantepec during Tehuantepecer events: a numerical study with WRF high-resolution simulations

Miguel A. Prósper<sup>1</sup>, Ian Sosa Tinoco<sup>2</sup>, Carlos Otero-Casal<sup>1,3</sup>, and Gonzalo Miguez-Macho<sup>1</sup>

<sup>1</sup>Universidade de Santiago de Compostela, Galicia, Spain.

<sup>2</sup>Technical Institute of Sonora, Sonora, Mexico.

<sup>3</sup>MeteoGalicia, Xunta de Galicia, Galicia, Santiago de Compostela, Spain

**Correspondence:** Miguel A. Prósper (prosper.miguelangel@gmail.com)

## Abstract.

Tehuantepecers or Tehuanos are extreme winds produced in the Isthmus of Tehuantepec, blowing south through the Chivela pass, the mountain gap across the isthmus, from the Gulf of Mexico into the Pacific Ocean. They are the result of the complex interaction between large-scale meteorological conditions and local orographic forcings around Chivela pass and occur mainly in winter months, due to cold air damming in the wake of cold fronts that reach as far south. Even though the name refers mostly to the intense mountain gap outflow, Tehuantepecer episodes can also generate other localized extreme wind conditions across the region, such as downslope windstorms and hydraulic jumps, strong turbulent flows that have a direct effect on the Pacific side of the isthmus and the Gulf of Tehuantepec.

This study focuses on investigating these phenomena using high horizontal and vertical resolution WRF (Weather Research and Forecasting) model simulations. In particular, we employ a four nested grid configuration, with up to 444 m horizontal spacing in the innermost domain and 70 hybrid-sigma vertical levels, 8 of which lie within the first 200 m above ground. We select one 36 hour period in December 2013, when favorable conditions for a strong gap wind situation were observed. The high-resolution WRF experiment reveals a significant fine-scale structure in the strong Tehuano wind flow, beyond the well known gap jet. Depending on the Froude number upstream the topographic barrier, different downslope windstorm conditions and hydraulic jumps with rotor circulations develop simultaneously at different locations east of Chivela pass with varied crest height. A comparison with observations suggests that the model accurately represents the spatially heterogeneous intense downslope windstorm and the formation of mountain wave clouds for several hours, with low errors in wind speed, wind direction, and temperature.

*Copyright statement.* TEXT

## 1 Introduction

The Isthmus of Tehuantepec, in the Mexican state of Oaxaca, is the narrowest stretch of land separating the Gulf of Mexico from the Pacific Ocean. The Sierra Madre mountains cross the isthmus from east to west, leaving, however, a pronounced gap in the middle (Chivela Pass), coinciding with the point of shortest distance between the two sea masses, of only 200 km. The elevation of the Chivela pass is 224 m, whereas mountain peaks in the side sierras reach 2000 m, creating ideal conditions to generate a powerful wind corridor (Romero-Centeno et al., 2003). In winter, cold high-pressure systems originating in North America move over the Gulf of Mexico in the wake of south-reaching cold fronts, and large pressure differences develop across the isthmus between the bay of Campeche and the Gulf of Tehuantepec, on the Pacific side. This pressure gradient results in a northerly wind situation, in which the flow is accelerated southward by cold air damming, traveling through Chivela Pass to finally blow violently outward into the Pacific Ocean, as it fans out and curves anticyclonically. This gap outflow extends for hundreds of kilometers over the Gulf of Tehuantepec, a result of the combined effect of the open marine surface and the low Coriolis parameter of the tropical latitude of the area. The small impact of planetary rotation yields very weak synoptic forcing; thus, the gap wind does not encounter any ambient large-scale flow to merge with, describing a very-close-to-inertial trajectory with a large radius, also as a consequence of the diminished Coriolis force (Steenburgh et al., 1998). In the Gulf of Tehuantepec, the strong sea surface wind stress generates intense upwelling and vertical mixing in the upper ocean (Hong et al., 2018). The largest number of these events tend to occur in December, with a mean duration of 48h (Brennan et al., 2010). These powerful mountain gap winds are called Tehuantepecers or Tehuanos, and have been the focus of several previous studies (Brennan et al., 2010; McCreary et al., 1989; Jaramillo and Borja, 2004) detailing their general setting, drivers and dynamics (Steenburgh et al., 1998) of strong wind situations in the isthmus. Little knowledge exists, however, on the fine-scale structure of the Tehuantepecer flow elsewhere across the Isthmus, away from Chivela pass. There is evidence from observations and earlier numerical studies (Steenburgh et al., 1998) that the low elevation topography of Chivela pass can excite mountain waves, and also that these are not only restricted to the pass itself but extend into the much higher mountain crests to the west and especially to the east, as the cold air pool is often thick enough to surpass them. This gravity wave activity can potentially result in downslope windstorms (DSWS hereafter) producing severe turbulent phenomena such as rotors and hydraulic jumps (HJ hereafter) (Durran, 1986a; Sheridan and Vosper, 2006) on the Pacific side of the isthmus, to the lee of local orography, which would explain several accidents related to strong winds reported by the Oaxaca's Civil Protection Commission (Santiago, 2018; Hernández, 2018; Televisa, 2018; Rodríguez, 2018) every year during some Tehuano occurrences. The ability to understand and forecast these events is very relevant, since the Isthmus has been an important development site for wind farms since the 2000's (Coldwell et al., 2017). Currently this region allocates 76.8% of the wind power capacity installed in Mexico, with approximately 2360 MW (Baxter et al., 2017), which is expected to double to 5076 MW by 2020 (AMDEE, 2018).

The main goal of the present work is to study the variability of flow behavior, beyond the well-known mountain gap jet, in Tehuano wind episodes across the isthmus of Tehuantepec, depending on topographic barrier height and thermodynamic conditions of the air mass, using high-resolution simulations with the Weather Research and Forecast (WRF) model. Many studies have successfully employed WRF to analyze this kind of mountain-flow events in other parts of the world. In the US,

for example, B. Pokharel et al. Pokharel et al. (2017b) study a DSWS and HJ to the lee of the Medicine Bow Mountains in southeast Wyoming. Another DSWS in this same area is also investigated by Grubišić et al. (2015) with WRF. Other studies such as Cao and Fovell (2016), Pokharel et al. (2017a), Prtenjak and Belusic (2009), Jung-Hoon and Chung (2006), Ágústsson and Ólafsson (2014), Priestley et al. (2017) also use WRF at high resolution to analyze mountain wave flows in different  
5 locations. To the best of our knowledge, there is not any previous work that studies in detail lee wave phenomena in the Mexican state of Oaxaca.

The high-resolution WRF simulations employed in the present study allow us to obtain a more complete knowledge of these events, from the synoptic scale to the **small scale**, focusing on the downslope winds and the HJ that develop **along the mountain ranges neighboring Chivela pass**. The article is organized as follows: in section II the methodology is explained in detail, from  
10 the climatology of the region to the model configuration. **In section III, the primary results obtained are shown, divided into synoptic-mesoscale situation and upstream-downstream structure of the phenomena**. Finally, in section IV the conclusions reached are discussed.

### **1.1 Mountain wave phenomena, hydraulic analog and relation with the Froude number**

**DSWSs** result from the intense flow acceleration occurring on the lee slope of a mountain under certain cross-barrier wind  
15 conditions. They resemble the behavior of water flow in an open channel when encountering an obstacle, such as when a relatively slow river increases its speed when flowing in a thin layer over a mill's dam or over a rock. As in the case of the river, **DSWSs** often end abruptly with a return to the state upstream of the obstacle through a turbulent HJ somewhere downstream. The similarity in both fluid's behavior suggests that the physical processes behind are also alike, and that shallow-water theory could be applied somehow to the atmosphere (Long, 1953). However, the complexity of the unbounded atmospheric flow,  
20 without a free surface, makes it difficult to make the analog so simple, because gravity waves in the atmosphere propagate vertically in addition to horizontally as in shallow water, and non-linear effects are important.

Considerable observational and numerical experiments have been developed to elucidate the dynamics of atmospheric mountain lee flows (see Durran (1990) for a review). The current view is that in the atmosphere, **DSWSs** are observed when stable air at low levels flows, similarly to shallow water, as like having a free surface somewhere above the obstacle preventing vertical  
25 energy dissipation. This occurs when gravity waves do not propagate vertically and break because of the presence of a critical level (Durran and Klemp, 1987) or due to overturning for having too large amplitude (Clark and Peltier, 1977), or when without wave breaking, there is an interface separating highly stable lower layers from less stable air above (Durran, 1986b; Klemp and Durran, 1987; Bacmeister and Pierrehumbert, 1988). **Wave breaking creates a well-mixed layer to the lee of the obstacle, which generates a dividing streamline separating undisturbed flow aloft and trapped energy and flow analogous to hydraulics in the lower surficial branch** (Smith, 1985b). A highly stable lower layer topped by less stable air results in reflecting and  
30 decaying waves aloft, enhanced non-linear effects, and the atmosphere also flowing like a two-layer fluid and behaving like shallow water when encountering the barrier.

**In shallow water theory, the Froude number (Fr), which is the ratio of the mean speed to the intrinsic gravity wave phase speed in the fluid, determines its behavior when encountering the obstacle, depending on whether gravity is balanced mostly**

by acceleration ( $Fr > 1$ ) or pressure gradient forces ( $Fr < 1$ ). HJs and significant flow acceleration to the lee of the obstacle occur when the fluid transitions from a subcritical ( $Fr < 1$ ) to supercritical ( $Fr > 1$ ) regime at the top of the barrier. It is not straightforward to define a Froude number to determine the regime of atmospheric flows (Sheridan and Vosper, 2006; Smith, 1989, 1985a) as it is for shallow water, because there is no clear analog to flow depth controlling gravity wave speed and pressure perturbations. Key factors determining wave properties and flow characteristics in this case are stratification, wind speed and barrier height, or rather, the relative values among them. A quantity that combines these three variables and is referred to as Froude number for shallow atmospheric flows over mountains by many authors, is the following (Smith, 1989):

$$Fr = \frac{U}{NH} \quad (1)$$

where  $U$  is the flow speed,  $N$ , the Brunt-Väisälä frequency (Equation (2)), and  $H$ , the mountain height.

$$N = \sqrt{\frac{g}{\theta_0} \frac{d\theta}{dz}} \quad (2)$$

with  $g$  the acceleration of gravity,  $d\theta/dz$ , the potential temperature gradient in the stable layer, and  $\theta_0$ , the potential temperature at the base of this layer. To avoid confusion with the classical Froude number, the inverse of  $Fr$  defined as above is often used instead and called the non-dimensional mountain height.  $Fr$  is a measure of flow deceleration and stagnation upwind from the mountain (Baines, 1987). It can also be regarded as an estimate of nonlinearity. When  $Fr \ll 1$  there are significant non-linear effects and blocking, whereas for  $Fr \gg 1$  the opposite occurs (Smolarkiewicz and Rotunno, 1989).  $Fr$  around 1 indicates a transitional regime between the two states and favorable conditions for the formation of DSWS and HJs.

## 2 Methodology

### 2.1 WRF Configuration

We use the Advanced Research WRF (ARW) model (Skamarock et al., 2008) version 3.9 (WRFV3.9) to perform the simulations. Based on a fully compressible and non-hydrostatic dynamic core, WRFV3.9 is a limited-area mesoscale and microscale model, with a terrain-following hydrostatic-pressure vertical coordinate, designed for operational forecasting, as well as research. For the experiments, we employ a nested domain configuration, in order to achieve sufficiently high resolution in the innermost grids to capture the small scale structure of the flow, while reproducing the synoptic phenomenology conducive to local DSWS in the parent one (Figure 1a).

The domain's configuration meets the requirements recommended by Warner (2011), including a parent (d01) and four nested grids (d02, d03, d04 and d05) (Figure 1a) one-way interacting. D01 is centered at 17.91 N and 93.44 W (Figure 1a) with 80 x 80 grid points of 36 km of horizontal resolution. The horizontal resolutions of d02, d03, d04, and d05 are: 12 km (91x91 grid points), 4 km (94x94 grid points), 1.3 km (103x103 grid points), and 444 m (106x106 grid points) respectively. D03 covers the whole isthmus area, with Chivela pass approximately in its center, while the highest resolution domains d04

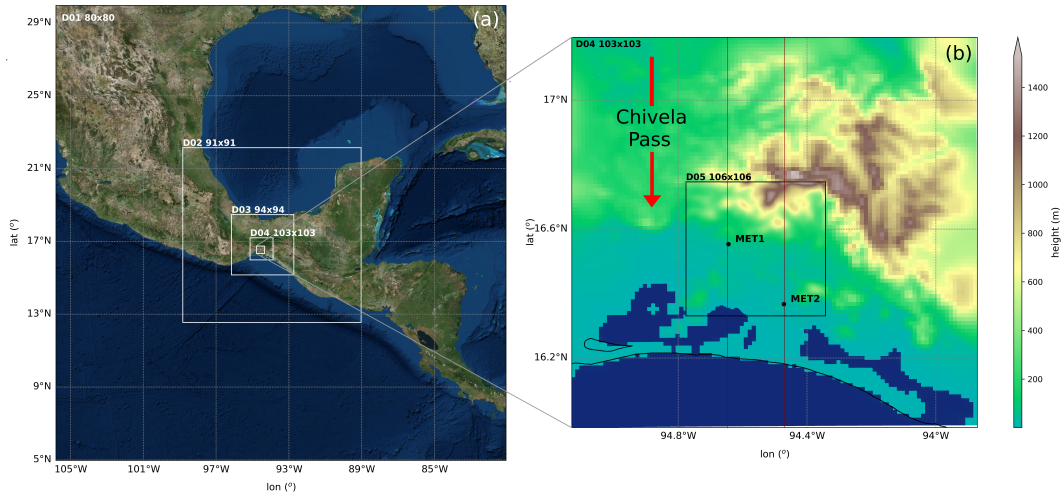


**Figure 1.** WRF nested domain configuration. (a) Coarser three domains with their number of grid points. (b) Higher resolution domains (d04 and d05), both with their respective topographies (m above sea level). MET1 and MET2 are the locations of the meteorological stations used as validation points. The two red lines represent the vertical cross-sections shown in Figures 3 and 5.

and d05 are slightly displaced to the south and east. D04 includes Chivela pass and the section of the Sierra Madre de Chiapas range east of it, with heights reaching about 2000m. For its part, the finest grid D05 encompasses the southernmost hills to the east of Chivela pass and the coastal plain at their base. This domain configuration focuses the area of interest of the study on the Pacific side of the Tehuano, encompassing the flow path before and after crossing the mountains, the exit section of the mountain gap and the gradually rising mountains east of it, around the only two available observational sites for validation, labeled as MET1 and MET2 in Figure 1b.

All the domains have 70 hybrid-sigma vertical levels, 8 of which lie within the first 200 m above ground, at about 16, 46, 71, 96, 122, 147, 173 and 198 m height. The hybrid sigma-pressure vertical coordinate follows the terrain near the surface and gradually transitions to constant pressure at higher levels. The benefit of this vertical coordinate system is a numerical noise reduction in the upper-layers over mountains (Powers et al., 2017). We maintain this fine vertical grid spacing in all the domains, to capture as wide a range of motions as possible over the depth of the boundary layer.

Land use information for d04 and d05 is obtained from the ESA CCI (European Space Agency Climate Change Initiative) database (Bontemps et al., 2013) with a resolution of 300 m. The terrain elevation used comes from the ASTER Global Digital Elevation Map (GDEM) from USGS (United States Geological Survey)(Slater et al., 2009) with a resolution of 30 m. In the other domains, terrain and land use data are from the WRF global standard database, both at 30'' resolution for d03 and 2' for d02 and d01.

We simulate a 36-hour period, from 2013-12-23 12:00 to 2013-12-25 00:00 UTC, which registers DSWS conditions in the observational data. Regarding the main physics options, the simulations use the tropical suite configuration (Table 1),

introduced in WRF version 3.9., except for the planetary boundary layer, which is parametrized by the Shin-Hong scale-aware scheme (S-H) (Shin and Hong, 2015). The next table summarizes this physics configuration used.

Microphysics	Hong and Lim (Hong and Lim, 2006)
Cumulus	Zhang and Wang. (Zhang et al., 2011) *disabled in d04 and d05
Long wave radiation	RRTMG (Iacono et al., 2008)
Short wave radiation	RRTMG (Iacono et al., 2008)
Planet boundary layer	Shin and Hong (Shin and Hong, 2015)
Surface layer option	Revised MM5 surface layer (Jiménez et al., 2012)
Land-surface physics	Noah land-surface (Tewari et al., 2004)

**Table 1.** Main physics parameterizations used.

The S-H planetary boundary layer option is more suitable for the high resolution of the innermost domain (444 m) because it helps to mitigate a double counting effect of the small-scale processes in gray-zone resolutions. Apart from this, this scheme provides a turbulent kinetic energy (TKE) diagnostic variable useful for our analyses.

## 2.2 Global model and real data

Global Forecast System (GFS) analysis data from the National Centers for Environmental Prediction (NCEP) is used as initial and boundary conditions for the WRF model, with a 3-h update interval. The horizontal resolution of this dataset for all variables is  $0.5^\circ \times 0.5^\circ$ , with 32 vertical levels ranging from 1000 to 10 hPa. The observational data used in this work is provided by the Mexican National Laboratory of remote sensors (<https://clima.inifap.gob.mx/lnmysr/Estaciones/MapaEstaciones>), collected every 15 minutes at two meteorological stations whose location is presented in Table 2 and marked in Figure 1b as MET1 and MET2. Wind speed, wind direction, and temperature at 3 m height from these points are used for validation.

	name	latitude (°)	longitude (°)	elevation (m)	height (m)
MET1	Santiago Níltepec	16.5535	-94.6439	65	3
MET2	Ixhuatan	16.3673	-94.4717	18	3

**Table 2.** Weather stations position

Model data are extrapolated from their native sigma levels to the height of the meteorological station using equation (3), which relates wind speed with friction wind speed, which is also a diagnostic variable in the model.

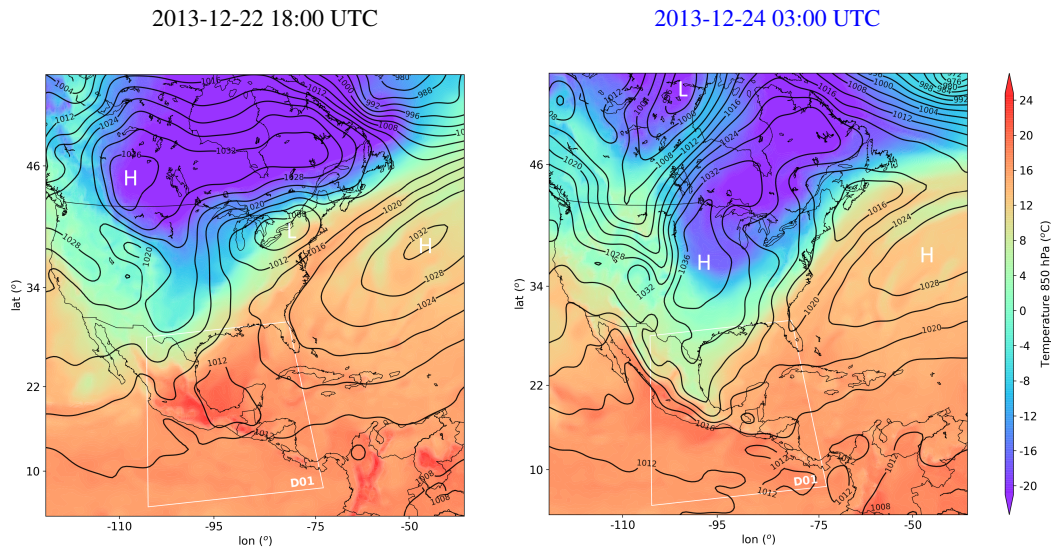
$$5 \quad ws_z = \frac{U_*}{K} \ln\left(\frac{z}{z_0}\right) \quad (3)$$

Where  $U_*$  is the friction velocity,  $K$  is the von Kármán constant,  $z$  is the height and  $z_0$  is the surface roughness (m).

### 3 Results and discussion

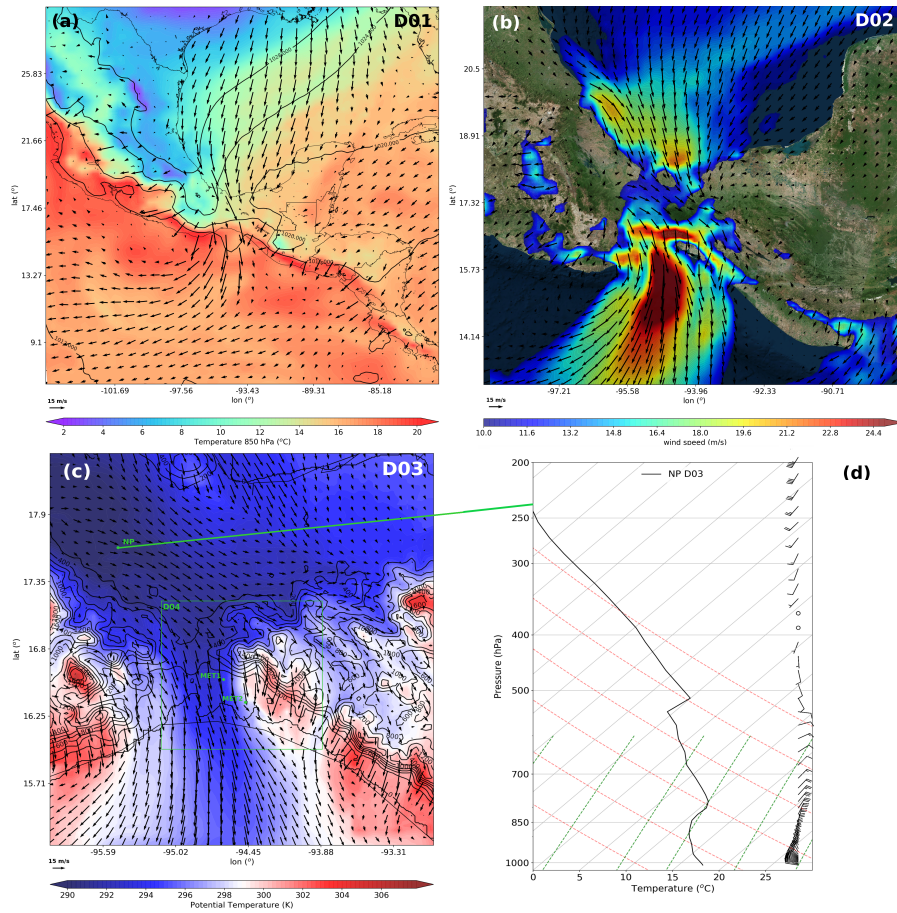
#### 3.1 Synoptic and Mesoscale situation

Figure 2 shows the synoptic situation, from GFS analysis data, in North and Central America 18 hours before (a) and at peak intensity of the event (b).



**Figure 2.** (a) 850 hPa temperature ( $^{\circ}\text{C}$ ) and sea level pressure (hPa) from GFS 0.5 Analysis data at 2013-12-22 18:00 UTC. (b) Same as (a) at 2013-12-24 03:00 UTC. D01 simulation domain is represented with a white square in both cases.

The large-scale setting is typical of Tehuantepecer wind episodes, where an Arctic air mass east of the Rockies pushes south across the Great Plains, with its leading edge reaching first the Gulf of Mexico (on December 22, Fig 2a) and then as far south as the bay of Campeche (about one day later, Fig. 2b), the result of cold air damming east of the Sierra Madre Oriental range in Mexico. The equatorward displacement of the associated high-pressure system on the wake of the cold front creates a strong pressure gradient across the Isthmus of Tehuantepec, ultimately producing the strong mountain gap winds through the low elevation of Chivela pass. The general situation favoring Tehuantepecer winds persists for about 6 days; more pronounced earlier on.



**Figure 3.** 2013-12-24 03:00 UTC (a) 850 hPa temperature ( $^{\circ}$  C), sea level pressure (hPa) and wind arrows in the parent grid d01, (b) wind speed (values $>10$  m/s) and wind arrows at  $\sigma=3$  (about 70m above ground) in d02, and (c) topography (m, contours) and potential temperature (K, shades) and wind arrows at  $\sigma=3$  in d03. (d) Skew-T log-P diagram on the Gulf of Mexico side of the Isthmus, northeast of Chivela Pass (NP point in (c), lat =  $17.6463^{\circ}$ , lon =  $-95.6246^{\circ}$ ) with wind barb profile at right.

Figure 3 shows the mesoscale conditions of the fully developed extreme wind episode at 03:00 UTC of 2013-12-24, from the WRF simulation. In the coarser grid D01 (36 km spacing, outlined in white in Figure 2) the cold air damming by the Sierra Madre Oriental mountains is clearly apparent, with the northerly cool air mass intrusion extending to the bay of Campeche, from where it is funneled across the Isthmus of Tehuantepec (Figure 3a). The higher resolution of the nested grids shows in greater detail the structure of the gap winds. Figure 3b, from the first nest D02 (12 km grid spacing), depicts the wind field (arrows) highlighting in shades the values above 10 m/s at about 70 m above the surface (sigma level 3), the approximate height of wind turbine hubs. The strong Tehuano outflow from Chivela pass reaches velocities of 25 m/s as it fans out for more than 100 km into the Pacific Ocean. High wind speeds are not only restricted to the outflow of the mountain gap itself; the simulation results suggest that they also occur in the mountains west and especially east of Chivela pass. The potential temperature field on

the same  $\sigma=3$  level at the enhanced resolution (4km) of the next nested grid D03 (Figure 3c) illustrates how the stable cold air mass to the north surmounts the lower hills neighboring the pass, particularly those to the east where elevation increases more gradually. As shown in the following section 3.2, acceleration on the top of these mountains and to their lee is related to gravity wave activity, which results in the development of strong downslope winds, rotors and HJs. The model sounding at location NP on the Gulf of Mexico side of the Isthmus (Figure 3d), shows in the temperature profile a stable lower boundary layer capped by a very stable isothermal layer from 850hPa up to about 2000 to 2500m, defining the depth of the cold air pool, indeed above the aforementioned mountain tops. A weak inversion associated with the subsidence within the high pressure system aloft is also clearly apparent just below 500hPa. Above this level, winds are weak and veer from being southeasterly to southwesterly in the upper troposphere. Below 500 hPa, winds back from an easterly to a northeasterly direction at about 800hPa, and more strongly in lower levels, becoming westerly at the surface, indicating intense cold air advection. There is a pronounced reverse wind shear in the lower troposphere.

As mentioned earlier, the only available observations in the area are from stations MET1 and MET2, whose positions are marked in Figure 3c. They are both located on the Pacific coastal plain, south of the mountains bordering Chivela pass to the east; MET1 closer to the relief and further west than MET2. The wind speed time series covering the entire Tehuano episode for both stations is shown in Figure 4. Wind speeds are low in the previous days and show a daily cycle, likely linked to sea breezes, more clearly evident in station MET2 closer to the coast. The situation changes after about December 23 at 6 UTC, when picking up intensity, wind speeds become more constant throughout the day, the signature of a Tehuano wind occurrence. At about 0 UTC on the 29<sup>th</sup>, the episode decays and winds go back to local breeze regimes. The extent of the simulated period covers the first 36h of the event (shaded in Fig.4), corresponding with its highest intensity in both locations. These observations away from Chivela pass show evidence, as the simulations suggest, that the neighboring mountains may also induce strong winds, even though they certainly do not reach out as far as the mountain gap outflow does.

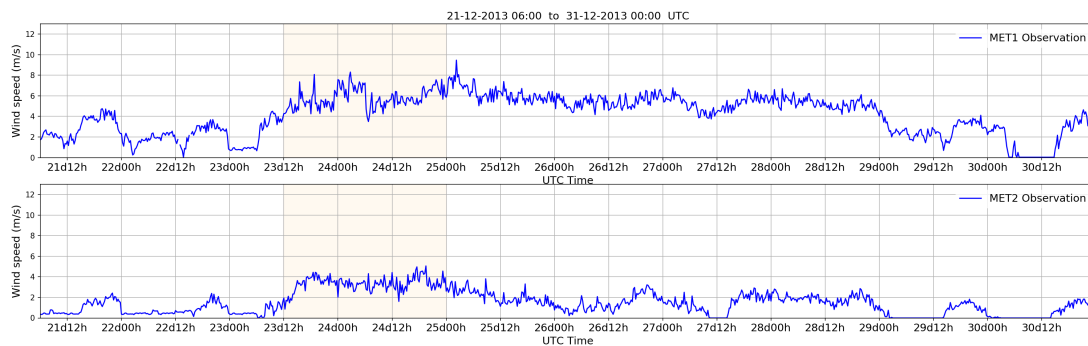


**Figure 4.** Wind speed (m/s) time series for observation stations MET1 and MET2 (locations marked in Figure 3). The orange shaded area corresponds to the period simulated.

### 3.2 Upstream-Downstream structure

In this section, we focus on the fine scale structure of the flow acceleration across the Isthmus, and more precisely, on that occurring on the westernmost section of the Sierra Madre de Chiapas mountains bordering Chivela Pass, apart from the well-known strong gap wind jet. This is the area covered by the d04 domain of 1.3 km resolution (highlighted in green in Fig. 3c), encompassing with 137 km from north to south the wind flow path before and after crossing the mountains. Figure 5 depicts from d04, latitudinal cross-sections (red lines in Figure 1b) facing east (south to the left, north to the right) of different variables at the longitude of the two validation points MET1 (Fig. 5a-f) and MET2 (Fig. 5g-l).

The tight isentropes on the windward side of the mountains (to the right in Fig. 5a, d, g and j), indicate a quite similar stable stratification in the whole lower tropospheric column in both cases; stronger in the layers below about 2.5 km and weaker above. The temperature profile in Fig. 3d evidences that the 2500m height level corresponds to the depth of the cold air. Winds are northerly in these lower layers to the north of the mountains, with somewhat higher speeds above 20m/s upstream from MET1 than further east, north of MET2. In both cases, winds above the cool pool are much weaker, and back to an easterly component at about 4000m and above. The latter height is therefore a critical level, since the cross-mountain flow component becomes null; thus, triggered gravity waves will break and dissipate when they approach it. Markowski and Richardson (2010) outline seven conditions conducive to DSWS, albeit not all of them absolutely necessary. These conditions are: (1) asymmetric mountain with steeper lee than windward side (Fig 5), (2) crossed by strong winds ( $> 15\text{m/s}$ ) (Fig 5), (3) mostly normal to the barrier (Fig.3, 5). (4) A stable layer above the top and less stable above that (Fig 3d, 6c), (5) with cold air advection and large-scale subsidence to maintain the stability (Fig 3d, 6c). Apart from this, (6) reverse wind shear above (Fig 3d, 6c) and (7) no cool pool in the lee (Fig 3a, 6b), is also desirable. These conditions are all perfectly met for both locations analyzed, as discussed previously, and indeed intense DSWSs occur in both cases.

The stably stratified cross barrier flow displays wave activity from early on, and wave breaking, as the vertical isentropes suggest (Fig. 5a and d), enhances turbulent mixing (Fig. 5c and f) and yields a region of weak stability and reverse flow immediately downwind from the mountain crests (Fig 5g and j). In both cases, isentropes on the windward side sink sharply under these layers of low stability on the lee side, much more pronouncedly for the tallest mountain (Fig. 5j). Encompassing the well mixed region to the lee, a split streamline develops (Smith, 1985b), and below its lower branch there is flow thinning and a significant increase in wind speed. The particular features existent on the lee side differ, however, depending of the height of the topographic obstacle. The strong accelerated flow confined by layers of strong wind shear and turbulence extends for many kilometers downwind from the lowest mountain (Fig 5i), while ending with a HJ and rotors at the foot when the barrier is higher (Fig 5j). The formation of either of these lee wave events is related to the Froude number upstream (Smith, 1989). We note that only the turbulence produced by the existent wind shear in the column is well captured in the simulation (Fig. 5i and l). The subgrid scale turbulence associated with gravity waves due to rotors and non-local turbulent advection or with instability resulting from wave overturning is not represented and accounted for, since a much higher horizontal and vertical resolution of the order of tens of meters would be needed in order to explicitly resolve these features (Vosper et al. 2018).

2013-12-23 15:00 UTC

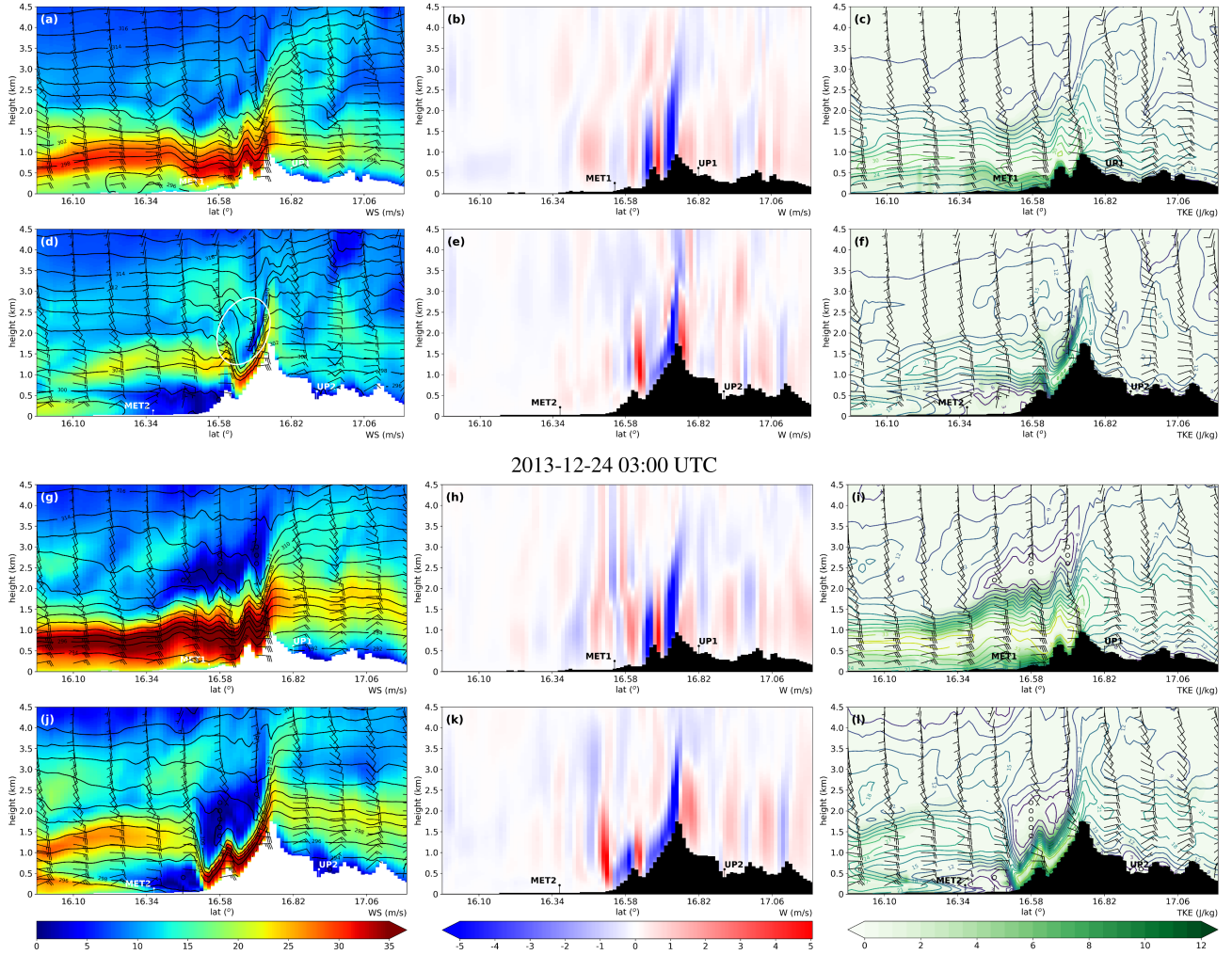


**Figure 5.** d04 vertical cross sections (a,d,g,j) potential temperature (K, contours), wind speed (m/s shades), and wind barbs referenced to the orientation of the cross section plane, (b,e,h,k) vertical wind component W (m/s) and (c,f,i,l) wind speed (m/s) isolines and turbulent kinetic energy (TKE, J/kg, shades). First (a,b,c) row for MET1 and second row (d,e,f) for MET2 correspond to the initial stages of the episode on 2013-12-23 15:00 UTC. Third row (f,h,i) at MET1 and fourth (j,k,l) row at MET2 are for the fully developed events on 2013-12-24 03:00 UTC. UP1 and UP2 are the locations where the Froude number upstream the mountain is calculated.

Figure 6a plots the Froude number (Equation 1), calculated using the average of the variables at sigma levels from the ground to the mountain top at upstream points UP1 (MET1 case), and UP2 (MET2 case). For the lowest mountain,  $Fr \approx 2$  during nighttime and even higher at some other times during the day, indicating supercritical conditions. The Brunt-Väisälä frequency around mountain top is between  $0.020$  and  $0.025 \text{ s}^{-1}$ . The generated mountain waves have relatively short wavelength and small amplitude and a modest **HJ** that propagates downstream can be seen at the initial stages of the episode at 15

UTC December 23 (Fig. 5a). 12 hours later, during nighttime, the aforementioned strong jet extending for tens of kilometers downwind is fully formed, with values above 35 m/s at about 750m above ground and strong turbulence at the surface and in the layers above the jet, where stability is much reduced. The temperature profile upwind (at 3 UTC December 24 and location UP1 in Fig 5) shows in the temperature profile a stable lower boundary layer capped by a very stable isothermal layer from 850hPa up to about 800hPa, or 2500m, defining the depth of the cold air pool. At the observation location MET1, downwind from the mountain, the lowest layers up to about 900 m are well mixed (slightly lower, up to 750m further downstream), the result of the intense surface turbulence. Above the latter height and up to about 1500 m elevation, a strongly stable layer exists corresponding with the aforementioned packing of the isentropes (and streamlines). This is where the highest wind speeds are found. **Stability is sharply reduced aloft**, in the region encompassed by the dividing streamline, and winds are rather weak and have an easterly component for the most part, parallel to the mountains.

For the higher mountain north of MET2,  $Fr \approx 1$  consistently in the period, indicating a critical flow regime, prone to the formation of HJs (Vosper2006 [5B]). The Brunt-Väisälä frequency **around mountain top** is between 0.012 and 0.015  $s^{-1}$  and the generated waves have higher amplitudes than in the MET1 case. Wave overturning and breaking is also much more pronounced (Fig 5d, **highlighted in white**) and the well mixed region **forming** to the lee of the crest is deeper. Isentropes and streamlines that sink underneath this region are packed in a very shallow layer on the lee slope of the mountain, generating an intense **DSWS** with speeds above 35 m/s at the surface. These strong winds end abruptly at the foot of the hill, where the flow transitions to subcritical conditions and a marked stationary **HJ** forms, with vertical wind speeds of 6 m/s. A rotor extending from the jump to the location of observation station MET2 is also evident in Fig. 5l. The temperature profile upstream is very similar to that of the MET1 case, but downwind from the mountain at location MET2, lacks the strongly stratified layer present in the case of the lower mountain. **We note that the soundings in Figure 6 show complex temperature profiles with discontinuous stratification in the planetary boundary layer, which underscores the importance of using high vertical resolution in simulations for these kind of studies.**

Results from the innermost nested grid d05 with the finest resolution (Fig 7) suggest that trapped lee waves develop in the MET1 case within the high stability layer where the strongest winds are found, just below the low stability region and the critical level aloft that prevent their vertical propagation. This wavelike pattern is a common feature in DSWS periods (Pokharel et al., 2017b; Hertenstein and Kuettner, 2005) and fully formed 12 h later (Fig. 7c), extends for more than 100 km downstream aligned with the general orientation in the northwest-southeast direction of the Sierra in the region. Waves are absent further east in the MET2 cross section, where the topographic barrier is higher and a stationary HJ forms instead, as discussed above.

Our results suggest that during Tehuano wind events, the Pacific side of the Isthmus of Tehuantepec east of Chivela pass is very prone to host extreme winds' phenomena. The formation of DSWSs in the area increases the impacts of the already strong mountain gap winds.

### 30 **3.3 Validation**

Finally, we contrast our simulation results with the very few data available for validation at meteorological stations MET1 and MET2. The two plots in Figure 8 compare the simulated wind speed (in d04 and d05) with observations from both stations.

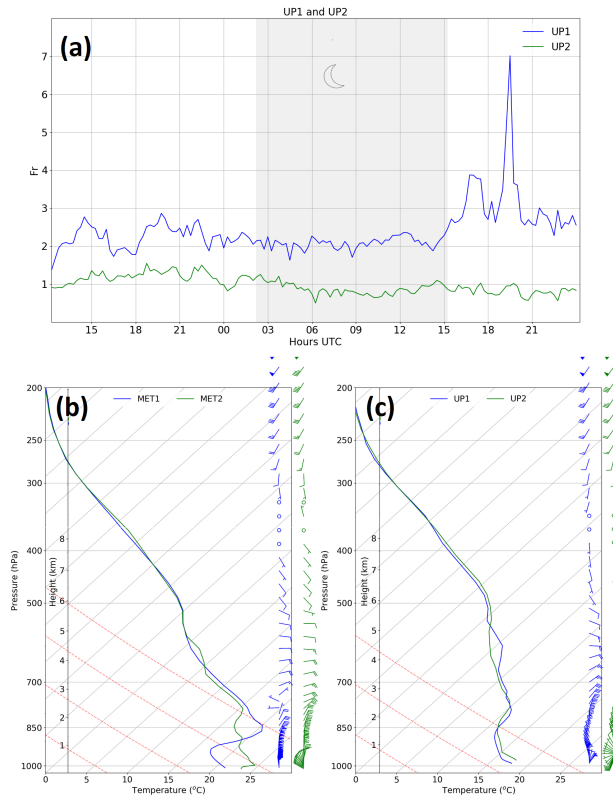


**Figure 6.** (a) Froude number upstream the mountain, north of MET1 (UP1) and of MET2 (UP2). The grey zone represents night time. (b) Skew-T log-P diagram at MET1 and MET2 and (c) at their corresponding upstream points UP1 and UP2. Wind barb profile for each pair of points at right.

Wind speed results from d04 and d05 at location MET1 are quite similar, and fare well with respect to observations (Figure 8a), slightly better in d05 case, with a mean absolute error (MAE) of 1.55 m/s (Table 2). The similarity in the low mean error between both simulations and their high correlation throughout the period are due to the nature of the event in that area, an intense and mostly steady jet that the d04 domain resolution (1.3 km) is already capable of resolving accurately. However, results in MET2, downwind from the strong HJ, present more differences between d04 and d05 (Figure 8b) and there is a significant improvement in d05 with respect to its parent domain d04. Wind speeds in d04 are overestimated (Mean error ME = 2.76 m/s), and present a daily cycle that is absent or very subtle in the observations. The complexity and fast variability of HJs formation in this area are better resolved in the higher resolution grid, which perhaps reproduces more accurately the stagnant flow and rotor formations downstream from the HJ. With regard to wind direction, errors are small for MET1 and significantly higher for MET2, due to the same reasons. As in the case of wind speeds, wind direction results from the finer grid d05 are

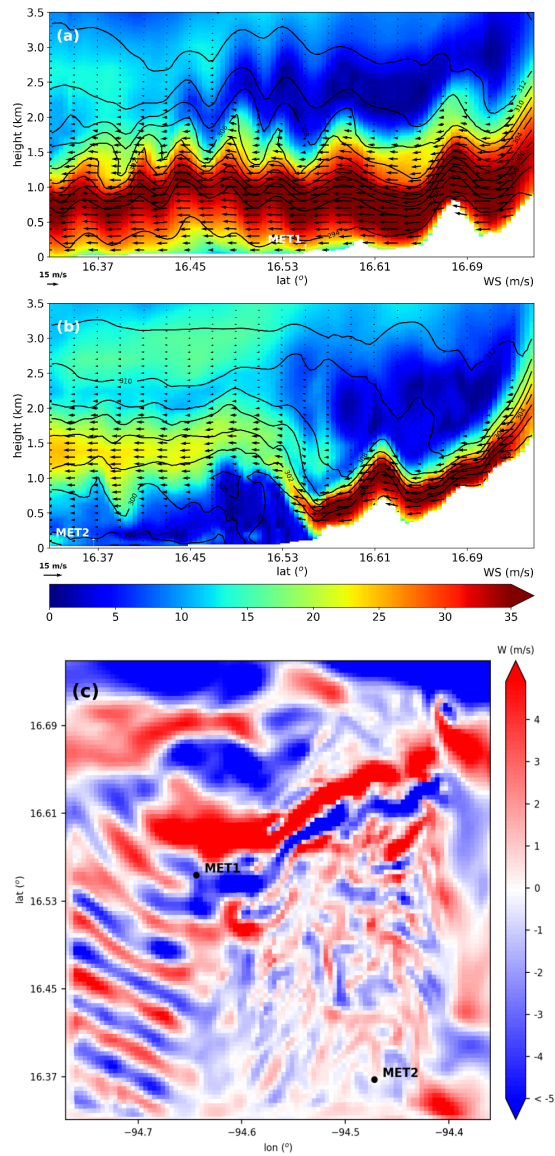


**Figure 7.** As in Fig. 5g and 5j but for d05, vertical cross sections of potential temperature (K, contours), wind speed (m/s shades), and wind barbs referenced to the orientation of the cross section plane at 2013-12-24 03:00 UTC for (a) MET1 and (b) MET2. (c) Vertical wind speed (m/s) in d05 at sigma level 17 (about 1400m above ground) when the trapped lee wave pattern in the region is fully formed at 15:30 UTC 2013-12-24.

also better than in d04. Temperature errors are equal or below 1 K in both locations and domains, hence the surface thermal  
 10 evolution is well captured.

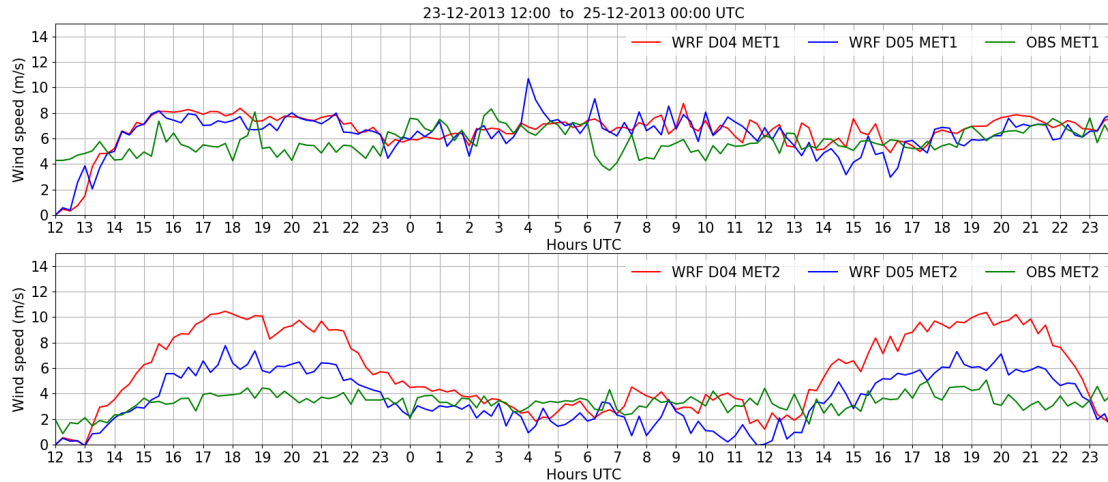


**Figure 8.** (a) Wind speed comparison among observations at MET1 (green), and model output from d04 (red) and, d05 (blue). (b) Same for station location MET2.

	<b>WS MAE</b> (m/s)	<b>WS ME</b> (m/s)	<b>WD MAE</b> (°)	<b>T MAE</b> (K)	<b>T ME</b> (K)
<b>MET1 D04</b>	1.82	1.26	16.15	0.85	-0.80
<b>MET1 D05</b>	1.55	0.80	13.63	0.77	-0.71
<b>MET2 D04</b>	2.76	2.35	27.87	0.71	0.01
<b>MET2 D05</b>	1.31	0.18	24.07	1.02	0.61

**Table 3.** Wind speed (WS), wind direction (WD), and temperature (T) mean errors (ME) and mean absolute errors (MAE) at MET1 and MET2 locations during the simulated period and for the two higher resolution domains (d04 and d05).

Lee waves can promote orographic cloud formation at different scales, depending on the amplitude of the wave and elevation (Armi and Mayr, 2011; Szmyd, 2016). Model results in d05 suggest that lenticular clouds form at the crests of the trapped lee waves depicted in Figure 7. Figure 9a shows a 3D representation of the modeled cloud water mixing ratio at 2013-12-24 15:30 UTC in d05. Cross sections of wind speed at the surface observation locations MET1 and MET2 as in Fig 5 and Fig 7 are also included for reference. A 2D view of the same cloud mixing ratio variable and wind arrows at sigma level 17 (about 1400 m above ground), revealing existing clouds, are depicted overlaying a satellite image of the area. An actual satellite image from Geostationary Operational Environmental Satellite - R Series (GOES-R) ([http://www.goes-r.gov/education/docs/fs\\_imagery.pdf](http://www.goes-r.gov/education/docs/fs_imagery.pdf)) around the same time is shown for comparison, indicating that remarkably similar mountain wave cloud formations were indeed observed in the area. The actual existence of these lenticular clouds with the same location and pattern as in the simulation further validates the model results.

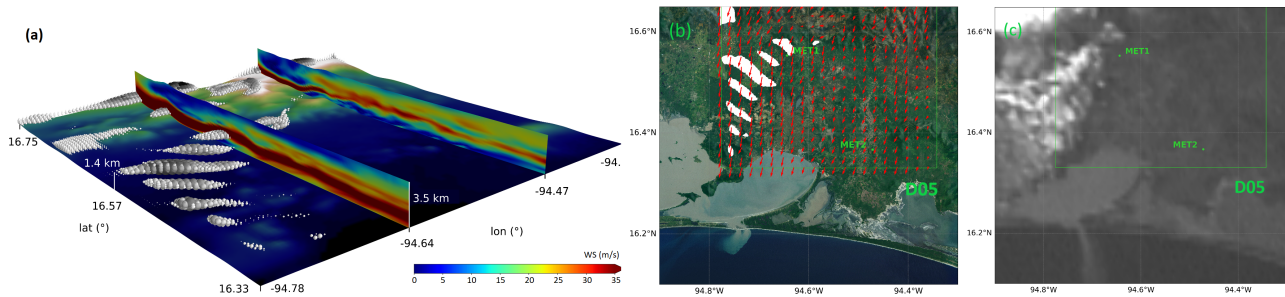


**Figure 9.** (a) Cloud water mixing ratio 3D representation in d05 at 2013-12-24 15:30 UTC. The two cross sections show the N-S wind profile at the longitudes of the meteorological stations MET1 and MET2. (b) Satellite image of the terrain in d05 and cloud water mixing ratio (white shades) and wind arrows at about 1.4 km above ground. (c) GOES-R satellite image on 2013-12-24 20:30 UTC, revealing very similar lenticular cloud formations at the same locations.

#### 4 Conclusions

In the present work, we studied lee wave phenomena occurring during Tehuano events on the Pacific side of the Isthmus of Tehuantepec using WRF high-resolution simulations. Orographic forcings at different scales result in the well-known gap wind jet off Chivela pass, but also in downslope windstorms and hydraulic jumps in the neighboring mountains. We analyzed these phenomena in an episode in December 2013 having the typical genesis of Tehuantepecer wind events. An Arctic air mass in North America pushed as far south as the bay of Campeche due to cold air damming east of the Rockies continuing to the east of the Sierra Madre Oriental range in Mexico. The displacement of the associated high-pressure system on the wake of the cold front created large pressure differences across the Isthmus of Tehuantepec, ultimately producing the strong mountain gap winds through the low elevation of Chivela pass. The model simulates these intense winds, blowing with speeds at the surface of more than 25 m/s that extend for many kilometers from the mountain gap, fanning out well into the Gulf of Tehuantepec, as it is commonly observed in Tehuano events (Steenburgh et al., 1998).

The depth of the cold surge on the coastal plains of the Gulf of Mexico side of the Isthmus is about 2500m, therefore thick enough to surmount the lower elevations to the west, and especially to the east of Chivela pass. The flow over these mountains results in intense DSWSs to their lee, with the generation of intense turbulence, HJs and rotors, depending on the particular height of the topography. We focus on two locations of different barrier elevation from where there are surface observations downwind: one of 963m closer to Chivela pass and another further east, with height increasing to 1736m

The thermodynamic characteristics of the air mass are rather uniform upwind of both mountains, with strong stability within the cool pool and weaker above, and intense northerly winds that back and weaken aloft to a more easterly component parallel to the barrier. The critical level where the cross-mountain wind component becomes zero, inhibiting wave propagation, is about 4000m. Mountain waves are generated in both cases, with smaller amplitudes for the lower mountain, where the Brunt-Väisälä frequency at crest height is between 0.020 and 0.025  $s^{-1}$ , than for the higher mountain, where the Brunt-Väisälä frequency is

about half. Wave breaking produces mixing and generates a region of low stability to the lee of the mountains, which is deeper where the waves have higher amplitude. The Froude number is around 2.5 at crest height in the lower barrier and the flow presents a supercritical behavior. The region of low stability to the lee of the mountain lies above about 1500m and leads to a packing of the isentropes and streamlines underneath, resulting in strong stability and flow acceleration. An intense jet develops with wind speeds of 35 m/s at about 750m above ground extending for tens of kilometers downwind from the mountains. Wind speeds are reduced closer to the surface due to intense turbulence. Trapped lee waves form at about 1500m, just below the well mixed layer aloft that prevents their vertical propagation. The Froude number decreases to about 1 further east as elevation rises and the flow presents a critical regime. Isentropes on the windward side of the mountain sink much more pronouncedly under the wider mixed layer generated by wave breaking to the lee, and are tightly packed in a shallow layer above the surface. This generates an intense wind storm on the lee slope of the mountain, with surface wind speeds up to 35 m/s. The accelerated flow down the mountain ends abruptly at its foot, where the flow turns to subcritical state and a marked stationary HJ forms, with vertical velocities of 6 m/s. A rotor circulation develops further downstream from the jump.

Only limited observations are available to validate our model results. Errors in surface wind speeds, directions and temperature are small at the only two stations available on the Pacific coastal plain downwind from the mountains. In addition, lenticular clouds similar in location and pattern to those produced by the model, are apparent in satellite imagery of the day of the event, providing valuable indication that the mountain lee wave phenomena simulated indeed correspond to a real scenario.

Our model results suggest that when the cold air mass intruding from the north on the Gulf of Mexico side of the Isthmus is thick enough to surmount the mountains, extreme wind events develop in the area during Tehuano events beyond the gap wind jet. These include DSWSs and HJs, which are intense and highly turbulent flows that can have a substantial impact on the existent wind farm industry in the region .

15 *Author contributions.* TEXT

*Competing interests.* TEXT

*Disclaimer.* TEXT

*Acknowledgements.* We would like to thank Mexican National Laboratory of remote sensors (INAFAP) (<http://clima.inifap.gob.mx/Inmysr/>) for the valuable real data provided, necessary to validate all the study. The model forecast simulations and development of the data analysis was performed at the Centro de Supercomputacion de Galicia (CESGA) (<http://www.cesga.es/>). Their computer facilities and support have been indispensable to carry out this project. Finally, we would like to acknowledge the Non-Linear Physics Group of Universidade de Santiago de Compostela (<http://www.usc.es/en/investigacion/grupos/gfnl>), which is where this whole project has been developed.

## References

- Ágústsson, H. and Ólafsson, H.: Simulations of Observed Lee Waves and Rotor Turbulence, *Monthly Weather Review*, 142, 832–849, <https://doi.org/10.1175/MWR-D-13-00212.1>, <http://journals.ametsoc.org/doi/abs/10.1175/MWR-D-13-00212.1>, 2014.
- 10 Armi, L. and Mayr, G. J.: The descending stratified flow and internal hydraulic jump in the lee of the Sierras, *Journal of Applied Meteorology and Climatology*, 50, 1955–2011, <https://doi.org/10.1175/JAMC-D-10-05005.1>, 2011.
- Bacmeister, J. and Pierrehumbert, R.: On high-drag states of nonlinear stratified flow over an obstacle, *Journal of the atmospheric sciences*, 45, 63–80, 1988.
- Baines, P. G.: Upstream blocking and airflow over mountains, *Annual review of fluid mechanics*, 19, 75–95, 1987.
- 15 Baxter, R., Hastings, N., Law, A., and Glass, E. J.: *Prospectiva de Energías Renovables 2017-2031*, Tech. Rep. 5, 2017.
- Bontemps, S., Defourny, P., Radoux, J., Van Bogaert, E., Lamarche, C., Achard, F., Mayaux, P., Boettcher, M., Brockmann, C., Kirches, G., Zülke, M., Kalogirou, V., Seifert, F., and Arino, O.: Consistent global land cover maps for climate modelling communities: current achievements of the ESA' and cover CCI, *ESA Living Planet Symposium 2013*, 2013, 9–13, 2013.
- Brennan, M. J., Cobb, H. D., and Knabb, R. D.: Observations of Gulf of Tehuantepec Gap Wind Events from QuikSCAT: An Updated Event  
20 *Climatology and Operational Model Evaluation, Weather and Forecasting*, 25, 646–658, <https://doi.org/10.1175/2009WAF2222324.1>,  
<http://journals.ametsoc.org/doi/abs/10.1175/2009WAF2222324.1>, 2010.
- Cao, Y. and Fovell, R. G.: Downslope Windstorms of San Diego County. Part I: A Case Study, *Monthly Weather Review*, 144, 529–552, <https://doi.org/10.1175/MWR-D-15-0147.1>, <http://journals.ametsoc.org/doi/10.1175/MWR-D-15-0147.1>, 2016.
- Clark, T. and Peltier, W.: On the evolution and stability of finite-amplitude mountain waves, *Journal of the Atmospheric Sciences*, 34,  
25 1715–1730, 1977.
- Coldwell, P. J., Ricardo, A., Quiroga, F., and Reyes, F. Z.: *Reporte de Avance de Energías Limpias 2017*, Tech. rep., 2017.
- Durran, D. R.: Another look at downslope windstorms. Part I: The development of analogs to supercritical flow in an infinitely deep, continuously stratified fluid, *Journal of the Atmospheric Sciences*, 43, 2527–2543, 1986a.
- Durran, D. R.: Another look at downslope windstorms. Part I: The development of analogs to supercritical flow in an infinitely deep,  
30 continuously stratified fluid, *Journal of the Atmospheric Sciences*, 43, 2527–2543, 1986b.
- Durran, D. R.: Mountain waves and downslope winds, in: *Atmospheric processes over complex terrain*, pp. 59–81, Springer, 1990.
- Durran, D. R. and Klemp, J. B.: Another look at downslope winds. Part II: Nonlinear amplification beneath wave-overturning layers, *Journal of the atmospheric sciences*, 44, 3402–3412, 1987.
- Grubišić, V., Serafin, S., Strauss, L., Haimov, S. J., French, J. R., and Oolman, L. D.: Wave-induced boundary-layer separation in  
35 the lee of the Medicine Bow Mountains. Part II: Numerical modeling, *Journal of the Atmospheric Sciences*, p. 150904104933002,  
<https://doi.org/10.1175/JAS-D-14-0376.1>, <http://journals.ametsoc.org/doi/abs/10.1175/JAS-D-14-0381.1>, 2015.
- Hernández, J.: *Motorista pierde la vida en accidente sobre carretera 190*, *El Imparcial de Istmo*, <http://imparcialoaxaca.mx/policiaca/245626/motociclista-pierde-la-vida-en-accidente-sobre-carretera-190/>, 2018.
- Hertenstein, R. F. and Kuettner, J. P.: Rotor types associated with steep lee topography: Influence of the wind profile, *Tellus, Series A: Dynamic Meteorology and Oceanography*, 57, 117–135, <https://doi.org/10.1111/j.1600-0870.2005.00099.x>, 2005.
- Hong, S. and Lim, J.: The WRF single-moment 6-class microphysics scheme (WSM6), <http://www.mmm.ucar.edu/wrf/users/docs/WSM6-hong{ }and{ }lim{ }JKMS.pdf>{ % }5Cn<http://search.koreanstudies.net/journal/thesis{ }name.asp?name=kiss2002{ }&key=2525908>, 2006.
- 5

- Hong, X., Peng, M., Wang, S., and Wang, Q.: Simulating and understanding the gap outflow and oceanic response over the Gulf of Tehuantepec during GOTEX, *Dynamics of Atmospheres and Oceans*, 82, 1–19, <https://doi.org/10.1016/j.dynatmoce.2018.01.003>, <https://doi.org/10.1016/j.dynatmoce.2018.01.003>, 2018.
- 10 Iacono, M. J., Delamere, J. S., Mlawer, E. J., Shephard, M. W., Clough, S. A., and Collins, W. D.: Radiative forcing by long-lived greenhouse gases: Calculations with the AER radiative transfer models, *Journal of Geophysical Research Atmospheres*, 113, 2–9, <https://doi.org/10.1029/2008JD009944>, 2008.
- Jaramillo, O. A. and Borja, M. A.: Wind speed analysis in La Ventosa, Mexico: A bimodal probability distribution case, *Renewable Energy*, 29, 1613–1630, <https://doi.org/10.1016/j.renene.2004.02.001>, 2004.
- 15 Jiménez, P. A., Dudhia, J., González-Rouco, J. F., Navarro, J., Montávez, J. P., and García-Bustamante, E.: A Revised Scheme for the WRF Surface Layer Formulation, *Monthly Weather Review*, 140, 898–918, <https://doi.org/10.1175/MWR-D-11-00056.1>, <http://journals.ametsoc.org/doi/abs/10.1175/MWR-D-11-00056.1>, 2012.
- Jung-Hoon, K. and Chung, I.-U.: Study on Mechanisms and Orographic Effect for the Springtime Downslope Windstorm over the Yeongdong Region Jung-Hoon, *Atmosphere*, 16, 67–83, 2006.
- 20 Klemp, J. and Durran, D.: Numerical modelling of Bora winds Numerische Modellierung der Bora, *Meteorology and Atmospheric Physics*, 36, 215–227, 1987.
- Long, R. R.: Some aspects of the flow of stratified fluids: I. A theoretical investigation, *Tellus*, 5, 42–58, 1953.
- Markowski, P. and Richardson, Y.: Mesoscale meteorology in midlatitudes, vol. 137, <https://doi.org/10.1002/qj.817>, <http://doi.wiley.com/10.1002/qj.817>, 2010.
- 25 McCreary, J. P., Lee, H. S., and Enfield, D. B.: The response of the coastal ocean to strong offshore winds: With application to circulations in the Gulfs of Tehuantepec and Papagayo, *Journal of Marine Research*, 47, 81–109, <https://doi.org/10.1357/002224089785076343>, <http://openurl.ingenta.com/content/xref?genre=article{&}issn=0022-2402{&}volume=47{&}issue=1{&}spage=81>, 1989.
- Pokharel, A. K., Kaplan, M. L., and Fiedler, S.: Subtropical Dust Storms and Downslope Wind Events, *Journal of Geophysical Research: Atmospheres*, 122, 10 191–10 205, <https://doi.org/10.1002/2017JD026942>, 2017a.
- 30 Pokharel, B., Geerts, B., Chu, X., and Bergmaier, P.: Profiling radar observations and numerical simulations of a downslope wind storm and rotor on the lee of the Medicine Bow mountains in Wyoming, *Atmosphere*, 8, <https://doi.org/10.3390/atmos8020039>, 2017b.
- Powers, J. G., Klemp, J. B., Skamarock, W. C., Davis, C. A., Dudhia, J., Gill, D. O., Coen, J. L., Gochis, D. J., Ahmadov, R., Peckham, S. E., Grell, G. A., Michalakes, J., Trahan, S., Benjamin, S. G., Alexander, C. R., Dimego, G. J., Wang, W., Schwartz, C. S., Romine, G. S., Liu, Z., Snyder, C., Chen, F., Barlage, M. J., Yu, W., and Duda, M. G.: The weather research and forecasting model: Overview, system efforts, and future directions, *Bulletin of the American Meteorological Society*, 98, 1717–1737, <https://doi.org/10.1175/BAMS-D-15-00308.1>, 2017.
- 35 Priestley, M. D., Pinto, J. G., Dacre, H. F., and Shaffrey, L. C.: The role of cyclone clustering during the stormy winter of 2013/2014, *Weather*, 72, 187–192, <https://doi.org/10.1002/wea.3025>, 2017.
- Prtenjak, M. T. and Belusic, D.: Formation of reversed lee flow over the north-eastern Adriatic during bora, *Geofizika*, 26, 145–155, <https://doi.org/10.1016/j.memsci.2006.03.045>, 2009.
- Rodríguez, Ó.: Viento provoca voladura de camión en Oaxaca, Milenio, <http://www.milenio.com/estados/viento-provoca-voladura-de-camion-en-oaxaca>, 2018.
- 5 Romero-Centeno, R., Zavala-Hidalgo, J., Gallegos, A., and O'Brien, J. J.: Isthmus of Tehuantepec wind climatology and ENSO signal, *Journal of Climate*, 16, 2628–2639, [https://doi.org/10.1175/1520-0442\(2003\)016<2628:IOTWCA>2.0.CO;2](https://doi.org/10.1175/1520-0442(2003)016<2628:IOTWCA>2.0.CO;2), 2003.

- Santiago, A.: Atendió Protección Civil más de 20 reportes en el Istmo por fuertes vientos, *El Imparcial de Istmo*, <http://imparcialoaxaca.mx/istmo/245475/atendio-proteccion-civil-mas-de-20-reportes-en-el-istmo-por-fuertes-vientos/>, 2018.
- Sheridan, P. F. and Vosper, S. B.: A flow regime diagram for forecasting lee waves, rotors and downslope winds, *Meteorological Applications*, 13, 179–195, <https://doi.org/10.1017/S1350482706002088>, 2006.
- Shin, H. H. and Hong, S.-Y.: Representation of the Subgrid-Scale Turbulent Transport in Convective Boundary Layers at Gray-Zone Resolutions, *Monthly Weather Review*, 143, 250–271, <https://doi.org/10.1175/MWR-D-14-00116.1>, <http://journals.ametsoc.org/doi/10.1175/MWR-D-14-00116.1>, 2015.
- Skamarock, W., Klemp, J., Dudhi, J., Gill, D., Barker, D., Duda, M., Huang, X.-Y., Wang, W., and Powers, J.: A Description of the Advanced Research WRF Version 3, Tech. Rep. June, NCAR, <https://doi.org/10.5065/D6DZ069T>, 2008.
- Slater, J. A., Heady, B., Kroenung, G., Curtis, W., Haase, J., Hoegemann, D., Shockley, C., and Tracy, K.: Evaluation of the New ASTER Global Digital Elevation Model, 77, 335–349, 2009.
- Smith, R. B.: On Severe Downslope Winds, American Meteorological Society, 1985a.
- Smith, R. B.: On severe downslope winds, *Journal of the atmospheric sciences*, 42, 2597–2603, 1985b.
- Smith, R. B.: Low Froude Number Flow Past Three-Dimensional Obstacles. Part I: Baroclinically Generated Lee Vortices, *Journal of the Atmospheric Sciences*, 46, 3611–3613, [https://doi.org/10.1175/1520-0469\(1989\)046<1154:LFNFPT>2.0.CO;2](https://doi.org/10.1175/1520-0469(1989)046<1154:LFNFPT>2.0.CO;2), [http://journals.ametsoc.org/doi/abs/10.1175/1520-0469\(1989\)046{%}3C1154:LFNFPT{%}3E2.0.CO;2](http://journals.ametsoc.org/doi/abs/10.1175/1520-0469(1989)046{%}3C1154:LFNFPT{%}3E2.0.CO;2), 1989.
- Smolarkiewicz, P. K. and Rotunno, R.: Low Froude number flow past three-dimensional obstacles. Part I: Baroclinically generated lee vortices, *Journal of the Atmospheric Sciences*, 46, 1154–1164, 1989.
- Steenburgh, W. J., Schultz, D. M., and Colle, B. A.: The Structure and Evolution of Gap Outflow over the Gulf of Tehuantepec, Mexico, *Monthly Weather Review*, 126, 2673–2691, [https://doi.org/10.1175/1520-0493\(1998\)126<2673:TSAE0G>2.0.CO;2](https://doi.org/10.1175/1520-0493(1998)126<2673:TSAE0G>2.0.CO;2), <http://journals.ametsoc.org/doi/abs/10.1175/1520-0493{%}281998{%}29126{%}3C2673{%}3ATSAE0G{%}3E2.0.CO{%}3B2>, 1998.
- Szmyd, J.: Influence of lee waves and rotors on the near-surface flow and pressure fields in the northern foreland of the Tatra Mountains, *Meteorological Applications*, 23, 209–221, <https://doi.org/10.1002/met.1546>, <http://doi.wiley.com/10.1002/met.1546>, 2016.
- Televisa, N.: Suspenden clases en escuelas del Istmo de Oaxaca por fuertes vientos, *NOTICIEROS TELEVISIA*, <https://noticieros.televisa.com/ultimas-noticias/clima-oaxaca-suspenden-clases-escuelas-del-istmo-por-viento/>, 2018.
- Tewari, M., Chen, F., Wang, W., Dudhia, J., LeMone, M. A., Mitchell, K., Ek, M., Gayno, G., Wegiel, J., and Cuenca, R. H.: IMPLEMENTATION AND VERIFICATION OF THE UNIFIED NOAH LAND SURFACE MODEL IN THE WRF MODEL, *Bulletin of the American Meteorological Society*, pp. 2165–2170, <https://doi.org/10.1007/s11269-013-0452-7>, 2004.
- Warner, T. T.: Quality assurance in atmospheric modeling, *Bulletin of the American Meteorological Society*, 92, 1601–1610, <https://doi.org/10.1175/BAMS-D-11-00054.1>, 2011.
- Zhang, C., Wang, Y., and Hamilton, K.: Improved Representation of Boundary Layer Clouds over the Southeast Pacific in ARW-WRF Using a Modified Tiedtke Cumulus Parameterization Scheme \*, *Monthly Weather Review*, 139, 3489–3513, <https://doi.org/10.1175/MWR-D-10-05091.1>, <http://journals.ametsoc.org/doi/abs/10.1175/MWR-D-10-05091.1>, 2011.